Reactivity of Novel High-performance Fuels on Commercial Three-way Catalysts for Control of Emissions from Spark-ignition Engines

Sreshtha Sinha Majumdar, Josh A. Pihl, Todd J. Toops*
National Transportation Research Center, Oak Ridge National Laboratory

Manuscript Text, Figures and Tables

*Corresponding author: Josh A. Pihl
pihlja@ornl.gov

This manuscript has been authored by UT-Battelle, LLC, under contract DE-AC05-00OR22725 with the US Department of Energy (DOE). The US government retains and the publisher, by accepting the article for publication, acknowledges that the US government retains a nonexclusive, paid-up, irrevocable, worldwide license to publish or reproduce the published form of this manuscript, or allow others to do so, for US government purposes. DOE will provide public access to these results of federally sponsored research in accordance with the DOE Public Access Plan (http://energy.gov/downloads/doe-public-access-plan).

Abstract

The Department of Energy "Co-Optimization of Fuels and Engines" initiative aims to simultaneously develop novel high-performance fuels with advanced engine designs to reduce petroleum consumption. To achieve commercialization, advanced engines running on alternative fuels still must meet emissions regulations. Warm three-way catalysts (TWC) are very effective at meeting the stringent emissions regulations on pollutants such as nitrogen oxides (NOx), non-methane organic gases (NMOG) and carbon monoxide (CO) from gasoline-fueled spark-ignition (SI) engines operating under stoichiometric conditions; thus, most SI engine emissions occur during cold-start, when the TWC has not yet achieved light-off. In the current study, the light-off behavior of novel high-performance fuel candidates has been investigated on a hydrothermally-aged commercial TWC using a synthetic engine-exhaust flow reactor system according to industry guidelines. Over 30 potential fuel components were examined in this study, including alkanes, alkenes, alcohols, ketones, esters, aromatic ethers, and non-oxygenated aromatic hydrocarbons. Short-chain acyclic oxygenates, including alcohols, ketones, and esters, tended to light off at relatively low temperatures, while alkenes, aromatics, and cyclic oxygenates tended to light off at relatively high temperatures. The light-off behavior of alkanes and alkenes depended strongly on their size and structure. In terms of the influence on CO light-off on the TWC, the fuels fell into two distinct categories: (i) non-inhibiting species including C_2-C_3 alcohols, alkanes, acyclic ketones, and esters; and (ii) inhibiting species including alkenes, aromatic hydrocarbons, cyclic oxygenates, and C_4 alcohols.

Keywords: Light-off, three-way catalyst, cold start, biofuel, hydrocarbon oxidation

1. Introduction

To reduce petroleum consumption, the U.S. Department of Energy (DOE) "Co-optimization of Fuels and Engines" initiative, also known as Co-Optima, aims to simultaneously develop novel high-performance fuels and advanced high efficiency engines. For spark-ignition (SI) engines, changes in certain fuel properties, particularly research octane number (RON) and octane sensitivity, and associated changes in engine design parameters provide proven pathways to improved fuel efficiency [1,2]. Co-Optima researchers have identified a number of potential fuel blendstocks that could provide the desired changes in fuel properties [3]. Many of the blendstocks could be derived from biomass, further reducing overall petroleum consumption and greenhouse gas emissions. However, high performance fuels and advanced engines will only achieve market acceptance if they do not jeopardize a vehicle's ability to meet emissions regulations. The goal of this investigation was to understand how changes in fuel chemistry might impact the performance of the emissions control system in vehicles powered by SI engines.

The stringent emissions regulations [4] in place for pollutants such as nitrogen oxides (NO_x), carbon monoxide (CO) and non-methane organic gases (NMOG) necessitate robust engine-exhaust aftertreatment systems. For SI engines in gasoline-fueled modern light-duty vehicles operating at nominally stoichiometric air to fuel ratios (AFR), precisely tuned three-way catalysts (TWC) are extremely efficient at meeting these rigorous emissions standards by reducing NO_x to nitrogen and oxidizing CO and NMOG to CO_2 and H_2O. However, TWCs are only effective when they are operating above a critical temperature (light-off temperature) [5]. When the engine is first started, the TWC is below the light-off temperature, and the regulated pollutants escape from the vehicle exhaust into the environment. These "cold-start" emissions occur for the first 60-120 s and have been found to account for ~80% of the total emissions during a typical drive cycle [6,7]. As these species have deleterious effects on the environment, including formation of photochemical smog and acid rain, these cold-start emissions are highly undesirable. Therefore, a novel fuel-component candidate must be evaluated in terms of its reactivity on commercial TWCs to ensure

that the abovementioned regulated pollutants do not slip into the environment from the exhaust under vehicle operating conditions.

Traditionally, propane and propene have been used as model hydrocarbon molecules representing low and high catalytic reactivity on TWCs, respectively [6,8,9,10]. Both of these hydrocarbons are gaseous at ambient conditions, so it is easier to introduce them into experimental setups compared to liquid species. There are examples of studies on catalytic oxidation of more complex organic compounds in the literature, including alcohols, ketones, esters and aromatics, but these are typically conducted in the presence of only oxygen or air and/or CO in the feed [11,12,13,14,15,16,17]. The simplified feed gas mixtures, especially those in which water vapor is absent mask the complexities involved in emission control catalysis wherein competitive adsorption of reactants on the catalyst and, consequently, competing reactions play an important role.

Moreover, while propane and propene tend to show the full range of HC oxidation activity for a particular catalyst formulation, the catalytic reactivity of specific fuel components will depend on their chemical structures. Cleavage of the weakest C-H bond in the molecule usually activates the molecule, resulting in the formation of radicals and intermediates which determine the subsequent catalytic reaction pathways leading to oxidation over the TWC [18,19]. Both the strength of the weakest C-H bond and the configuration of the reaction intermediates depend on the structure of the starting fuel molecule, especially the functional groups contained in the molecule.

The importance of investigating the effect of the hydrocarbon structure on the catalytic reactivity of the fuel is further exemplified by the structure-reactivity relationships of selected alkanes, alkenes and alkyl-/polyalkyl-benzenes (6-20 carbon atoms) reported by Diehl et al. [20] on a Pt/Al_2O_3 catalyst. McCabe and co-workers' studies on specific single-component fuel emissions from a pulse flame combustor and their conversions over a TWC under isothermal conditions [21] highlighted the differences in reactivity of a hydrocarbon on a TWC based on their structure. The fast-light off experiments capturing the differences in reactivity of selected hydrocarbons on TWCs during cold-start reported by Bäroth et al. [6] further emphasized the inability

of model hydrocarbons such as propane and propene to accurately reveal the catalytic reactivity and inhibitive effects of a fuel on CO light-off. Poulopoulous and co-workers [22] have also examined the TWC conversion efficiency for hydrocarbon emissions under different engine operating conditions. More recently, Kang and co-workers [23] have reported the reactivity of speciated hydrocarbons on crushed commercial Pd and Rh based TWCs in the presence of a full engine-exhaust gas mixture and have also emphasized the role of hydrocarbon structure on its catalytic reactivity.

This contribution presents the results from catalytic light-off studies on a hydrothermally-aged commercial TWC using a synthetic engine-exhaust flow-reactor as a means to capture fuel-composition effects on emissions control for a spark-ignited light-duty vehicle. Investigations into the reactivity of potential novel high-performance fuel candidates including oxygenated hydrocarbons with bio-origins as well as petroleum-derived fuels from several functional groups (including alcohols, ketones, esters, aromatic ethers, aromatic hydrocarbons, alkenes and alkanes) have been conducted. A simple surrogate mixture designed to represent commercially available gasolines containing 10% ethanol (denoted E10, and consisting of 10% ethanol, 25% toluene, and 65% iso-octane by liquid volume) was also included in the light-off investigations. Fuel components that light off later (at higher temperatures) than the E10 surrogate may create new challenges in meeting current and future emissions control regulations. These potential challenges need to be considered in the overall evaluation of potential high-performance fuel blendstocks within the Co-Optima initiative. The concerted effort into examining the light-off profiles of a wide range of potential fuel components on a commercial TWC under full synthetic engine-exhaust feed conditions also provides a foundation for ongoing investigations into the light-off behavior of multi-component fuel blends representative of real-world fuels.

2. Experimental Methods

2.1. Three-way catalyst (TWC) specifications

The three-way catalyst (TWC) used for evaluating the light-off behavior of the different fuel components under consideration is a commercial TWC from a model year (MY) 2009 Chevrolet Malibu super ultra-low emission vehicle (SULEV)/partial

zero emission vehicle (PZEV). The TWC is dual-zoned with a Pd-rich front zone and a Pd/Rh/CeO_2 rear zone. The Pd and Rh content in both zones of the TWC is shown in Table 1. Core samples (2.0 cm diameter by 2.5 cm long) were cut from both zones of the TWC monolith and loaded in tandem in the flow reactor, with the rear zone core placed directly behind the front zone core.

Table 1: Pd and Rh content on the dual-zone Chevrolet Malibu Three-way catalyst

Three-way Catalyst	Pd (g/L)	Rh (g/L)
Front zone	7.3	0
Rear zone	1.1	0.3

2.2. Hydrothermal aging protocol

Prior to testing the TWC, it was hydrothermally aged as per industry guidelines delineated in the U.S. DRIVE "Low-Temperature Oxidation Catalyst Test protocol" [24] for stoichiometric gasoline direct injection (S-GDI) exhaust applications. The TWC was aged for 50 h at 800°C under neutral-rich-lean cycles of 1 min duration. The gas composition and duration for each condition is detailed in Table 2.

Table 2: Gas composition for hydrothermal aging the catalyst *

Mode	Duration (1 min total)	Gas composition (Balance N_2)				
		[O_2] %	**[CO_2] %**	**[H_2O] %**	**[CO] %**	**[H_2] %**
Neutral	40 s	-	10	10	-	-
Rich	10 s	-	10	10	3	1
Lean	10 s	5	10	10	-	-

* S-GDI conditions in the LTOCT protocol

2.3. Experimental set-up details

Catalyst light-off measurements were conducted on an automated synthetic exhaust flow reactor similar to one described previously [25] and depicted in Figure 1. Metal-sealed mass flow controllers (MKS Instruments) were used to meter the flow of

gaseous species from compressed gas (or cryogenic liquid) cylinders (AirGas) to generate gas mixtures with the desired composition. Water was introduced through a custom vapor delivery system consisting of: an HPLC pump (Eldex Laboratories); a liquid preheater made from a 1.6 mm outer diameter (OD) 1 m long stainless steel tube wrapped around a 9.5 mm diameter cartridge heater; and a stainless steel capillary (1.6 mm OD, 0.18 mm ID, 50 mm long) that injected the water vapor into a 200 °C inert gas stream. The liquid fuels, purchased from Sigma Aldrich, were stored in a reservoir pressurized under N_2 and fed into a Bronkhorst vapor delivery module. The vaporized fuel was then added to the gas stream comprising 13 % H_2O, 13 % CO_2, 1670 ppm H_2, 5000 ppm CO, 1000 ppm NO and O_2 such that the total hydrocarbon concentration in the reaction feed mixture was equivalent to 3000 ppm (C_1). The O_2 concentration was varied to adjust λ which is defined as: $AFR/AFR_{stoic.}$. The feed conditions and synthetic engine-exhaust gas composition are based on the U.S. DRIVE "Low-Temperature Oxidation Catalyst Test protocol" [24] for stoichiometric gasoline direct injection (S-GDI). All of the reactor gas lines (6.4 mm OD) were heated to roughly 200 °C to prevent condensation or adsorption of reacting species.

The catalyst core sample was wrapped in non-woven alumina tape (Cotronics) and loaded in a 25 mm OD quartz tube (Quartz Scientific). The upstream portion of the quartz tube was filled with 3 mm OD 1 mm ID quartz tubes to increase heat transfer to the inlet gas stream and improve temperature uniformity. The 25 mm quartz tube was fitted with graphite ferrules and custom stainless steel end caps that connected to the reactor gas lines and provided inlet ports for thermocouples and pressure transducers. The quartz tube assembly was placed inside two side-by-side tube furnaces (Lindberg Blue/M) to preheat the gases fed to the catalyst sample. The catalyst core sample was located just outside the heated zone of the second furnace. Type K thermocouples (0.5 mm diameter) were deployed 5 mm upstream, 5 mm downstream, and at the midpoint inside the catalyst core sample to monitor catalyst temperatures. Reactor pressures were monitored with silicon-diaphragm absolute pressure transducers (Omegadyne). Inlet and outlet gas compositions were measured with a Flame Ionization Detection (FID) Hydrocarbon Analyzer (California Analytical), a Multigas 2030HS FTIR spectrometer (MKS Instruments), and a PrismaPlus

quadrupole mass spectrometer (Pfeiffer). A custom LabVIEW (National Instruments) interface provided automated data acquisition and system control.

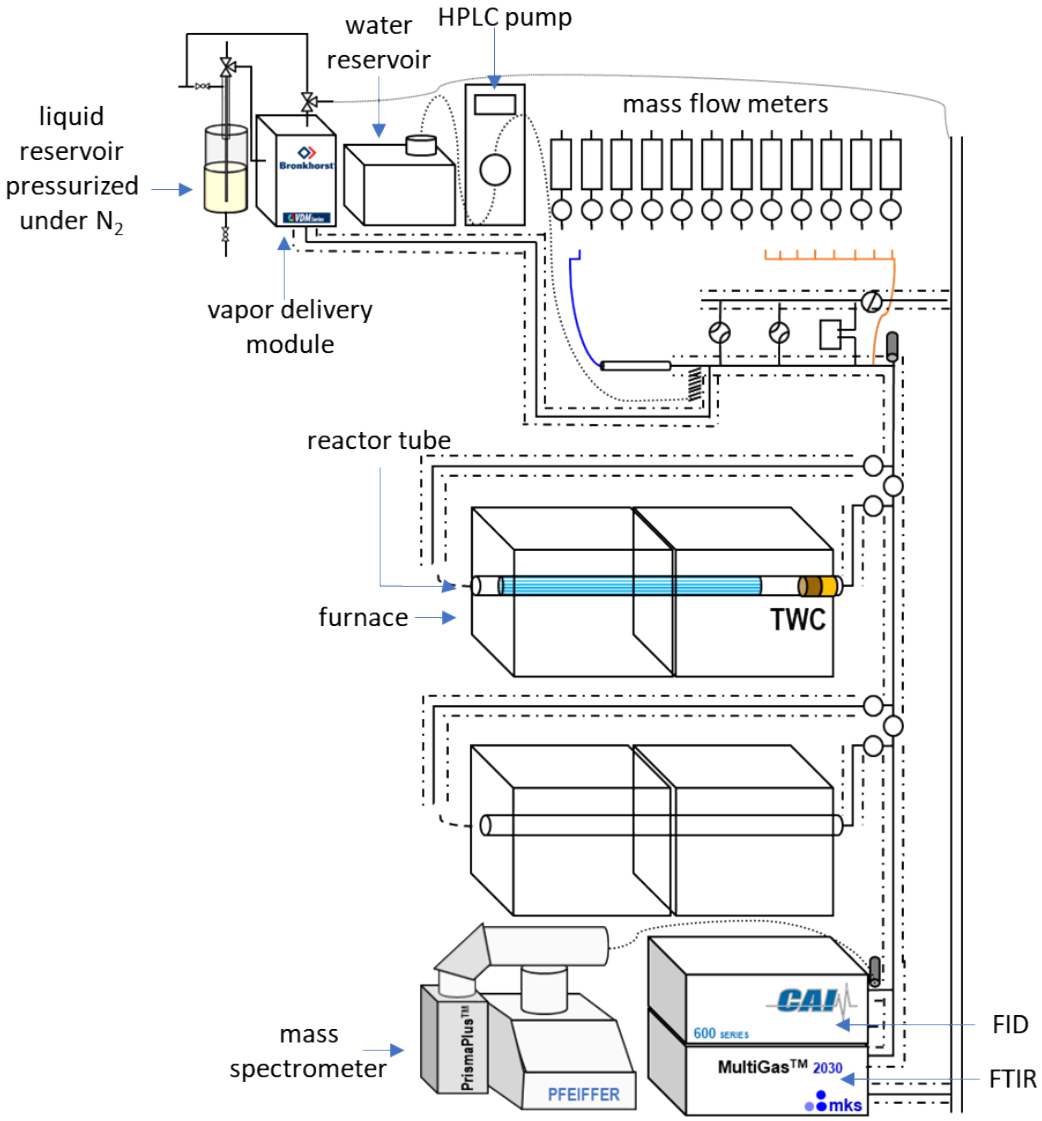

Figure 1: Schematic of the synthetic exhaust flow reactor system

2.4. Experimental protocol

The TWC was de-greened in the presence of 10 % CO_2 and 10 % H_2O for 4 h at 700 °C before conducting the catalyst light-off experiments. The experimental procedure followed for the catalytic light-off experiments is a modified version of the

standard SGDI light-off protocol [24]. The gas compositions for each step of the protocol are shown in Table 3.

Table 3: Gas composition for fuel light-off on TWC *

Step	Temperature °C	Gas composition (Balance N_2)						
		[O_2] %	**[CO_2] %**	**[H_2O] %**	**[CO] ppm**	**[H_2] ppm**	**[NO] ppm**	**[HC] ppm C_1**
Pretreatment	600	-	13	13	-	-	-	-
Light-down (gaseous HC)	500 to 100	0.72	13	13	5000	1670	1000	3000
Light-off (specific fuel)	100 to 500	Varied	13	13	5000	1670	1000	3000

* S-GDI conditions in the U.S.DRIVE Low Temperature Oxidation Catalyst Test Protocol

For each fuel light-off experiment, the catalyst is first pre-treated at 600 °C under neutral conditions. The catalyst is then cooled to 500 °C at which point the gaseous hydrocarbon (HC) mixture is introduced into the reactor along with O_2, CO_2, H_2O, CO, and NO. Light-down is conducted by cooling the TWC from 500 °C to 100 °C at ~5 °C/min (the furnace ramp rate slows as the temperature approaches 100 °C) in the presence of a gaseous HC mixture (150 ppm C_3H_8, 500 ppm C_3H_6 and 525 ppm C_2H_4). The gaseous HC light-down is conducted to ensure that the initial state of the catalyst before specific fuel light-off is consistent between the runs and to determine if the catalyst performance is deteriorating with time. At 100 °C, the flow of the gaseous HC mixture is terminated, and the reactor is flushed under neutral conditions. Then 3000 ppm C_1 equivalent of the specific fuel is introduced as part of the full synthetic engine-exhaust gas composition. The TWC is then heated from 100 °C to 500 °C at 5 °C/min and the catalyst light-off measurements are taken. For each fuel considered in this study, the experimental steps including pretreatment, gaseous HC light-down and specific fuel light-off are repeated three times to ensure reproducibility of results. The fuels investigated in this study include bio-derived oxygenated fuels such as the alcohols, ketones, esters and aromatic hydrocarbons and petroleum-derived non-oxygenated fuels such as alkanes and alkenes. The details of the fuels in this

investigation are listed in Table 4 along with their chemical structures and the temperatures at which 90% of the fuel component was converted over the TWC (T_{90}).

Table 4: Hydrocarbon structure and T_{90} summary

Functional Group	Structure	% O_2 (λ=0.999)	T_{90} ± error °C
Alcohols	ethanol	0.71	276 ± 4
	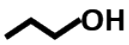 n-propanol	0.71	248 ± 5
	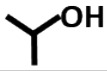 iso-propanol	0.71	219 ± 10
	n-butanol	0.71	283 ± 0.1
	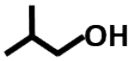 iso-butanol	0.71	282 ± 1
Ketones	2-butanone	0.68	255 ± 4
	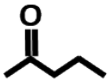 2-pentanone	0.68	249 ± 5
	cyclopentanone	0.65	281 ± 8
	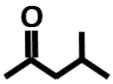 methylisobutylketone	0.69	250 ± 9
Esters	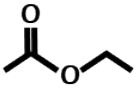 ethyl acetate	0.64	247 ± 2
	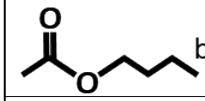 butyl acetate	0.66	248 ± 1
	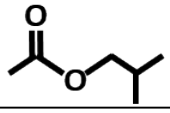 iso-butyl acetate	0.66	247 ± 3

Table 4: Hydrocarbon structure and T_{90} summary contd.

Functional Group	Structure		% O_2 (λ=0.999)	T_{90} ± error °C
Aromatic Ethers	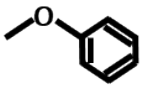	anisole	0.63	270 ± 0.2
	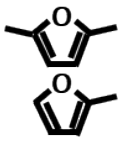	2,5-dimethylfuran 2-methylfuran	0.63	285 ± 1
Non-oxygenated aromatic hydrocarbons		toluene	0.65	262 ± 3
		m-xylene	0.66	277 ± 9
	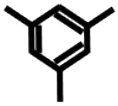	mesitylene	0.66	342 ± 14
Alkenes		ethene	0.71	209 ± 0.4
		propene	0.71	277 ± 0.3
		1-hexene	0.71	288 ± 1
		1-octene	0.71	298 ± 3
	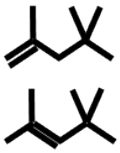	diisobutylene	0.71	275 ± 10
Alkanes	CH_4	methane	0.86	--
		propane	0.76	404 ± 3
		n-heptane	0.74	261 ± 1
		n-octane	0.73	242 ± 2
	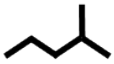	2-methylpentane	0.74	311 ± 7
		iso-octane	0.73	319 ± 12
		methylcyclohexane	0.71	255 ± 2
		methylcyclopentane	0.71	276 ± 3

3. Results and Discussion

3.1. Gaseous hydrocarbon mixture light-off

Prior to evaluations with liquid fuel components, the efficiency of the TWC in converting gaseous hydrocarbons such as ethene, propene and propane, as part of the synthetic exhaust feed was evaluated under stoichiometric conditions (λ=1). This data, shown in Figure 2, is included here to allow benchmarking of the aged commercial TWC sample relative to other formulations that are evaluated using the same protocol. More detailed discussions of the light-off behavior of the individual components included in the protocol mixture are included in subsequent sections.

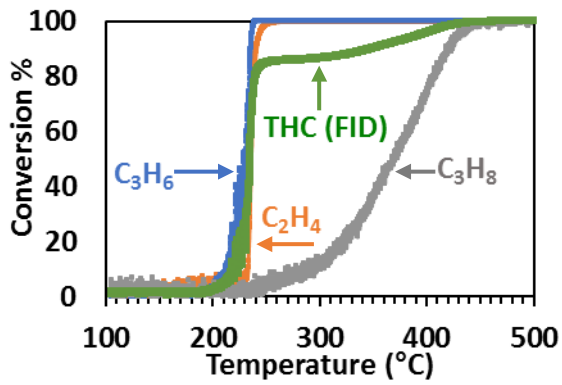

Figure 2: Gaseous hydrocarbon mixture light-off (THC (FID)) consisting of C_2H_4, C_3H_6 and C_3H_8 on a hydrothermally-aged commercial TWC. Feed conditions: 0.74% O_2, 13% CO_2, 13% H_2O, 5000 ppm CO, 1000 ppm NO, 1670 ppm H_2, 525 ppm C_2H_4, 500 ppm C_3H_6, 150 ppm C_3H_8.

3.2. Lambda (λ) sweep with E10 surrogate fuel

Prior to delving into the light-off study for the different fuel components, we conducted a lambda sweep on the hydrothermally aged TWC using the E10 surrogate fuel (which generated 230 ppm C_8H_{18}, 138 ppm $C_6H_5CH_3$, and 100 ppm C_2H_5OH in the synthetic exhaust mixture) by varying the oxygen concentration. We observed that, on increasing the O_2 concentration from 0.64% to 0.72% and consequently changing the λ from 0.995 to 0.999, the total hydrocarbon conversion increased. Figure 3 shows that as we go to richer conditions (λ<<1), due to an oxygen deficient environment, it gets more difficult to completely convert the hydrocarbons. For our studies, therefore,

we have selected λ=0.999 and have kept this constant for all the fuels under consideration. Since some of the fuel components included in the study contain oxygen, the O_2 concentration in the synthetic exhaust mixture was adjusted to maintain a lambda of 0.999. The O_2 concentrations used for each fuel component are summarized in Table 4. While careful consideration was given to maintaining consistent lambdas in the synthetic exhaust flow reactor experiments conducted for this study, such adjustments would be handled automatically on a vehicle through carefully calibrated engine control strategies that utilize feedback control based on exhaust oxygen sensors.

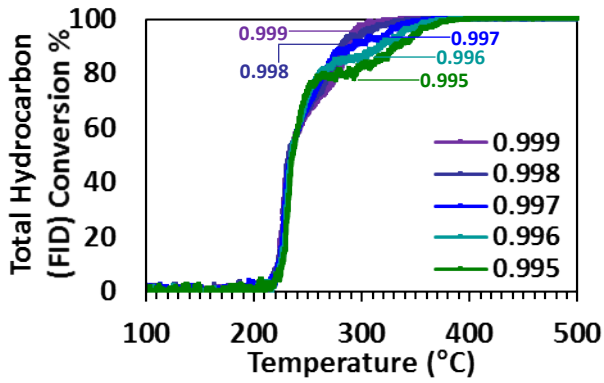

Figure 3: Comparison of total hydrocarbon conversion of E10 surrogate fuel between catalyst inlet temperature of 100-500°C when lambda (λ) is adjusted from 0.995 to 0.999 by varying O_2 concentration. Feed conditions: 0.64%-0.72% O_2, 13% CO_2, 13% H_2O, 5000 ppm CO, 1000 ppm NO, 1670 ppm H_2, 230 ppm C_8H_{18}, 138 ppm $C_6H_5CH_3$, 100 ppm C_2H_5OH.

The "total hydrocarbon (FID) conversion" label on the y-axis of Figure 3, and all subsequent figures containing light-off data, is there to highlight the fact that the calculated conversions are based on measurements from a FID, which measures total hydrocarbons in the exit stream from the three-way catalyst on a C_1 basis. The FID measurement captures both unreacted fuel components as well as most organic species formed from catalytic transformations of the fuel besides oxidation to CO and CO_2. This approach is more accurate and relevant than relying on measurements of disappearance of the fuel species through other analytical instrumentation such as gas chromatographs (GC) or Fourier transform infrared (FTIR) spectrometers.

3.3. Light-down with gaseous hydrocarbon mixture

To make sure that the initial state of the catalyst is comparable between the replicate runs, and to confirm that there is no long term degradation of the TWC performance, we conducted the ramp-down portion of the U.S. DRIVE protocol (during which the catalyst is cooled to the starting temperature under a full synthetic exhaust mixture) with the gaseous hydrocarbon mixture discussed in section 3.1.

The temperatures at which 50% (T_{50}) and 90% (T_{90}) of the gaseous hydrocarbons are converted are shown in Figure 4 for all runs conducted in this study. The error bars in Figure 4 were calculated from the three replicates conducted with each fuel component. The consistency of the measured light-down temperatures with the gaseous hydrocarbons over the 93 separate experiments conducted for this study show that the TWC performance is stable and the catalyst is not being degraded by the intervening light-off measurements. Therefore, the differences in the specific fuel light-off temperatures presented in subsequent sections are not affected by any change in the catalytic efficiency of the TWC, and are due to intrinsic differences in the reactivity of the fuel components.

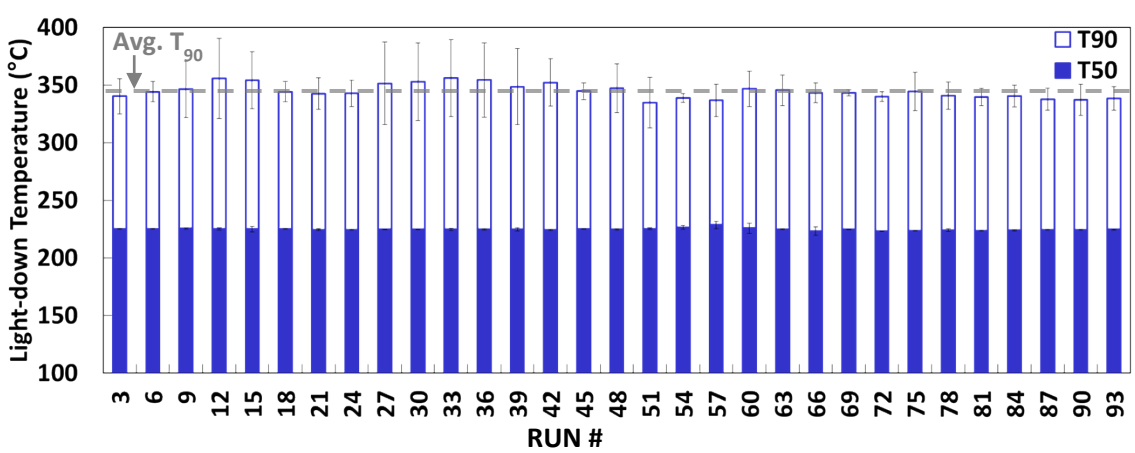

Figure 4: Gaseous hydrocarbon mixture light-down (THC (FID)) consisting of C_2H_4, C_3H_6 and C_3H_8 on a hydrothermally-aged commercial TWC. Feed conditions: 0.74% O_2, 13% CO_2, 13% H_2O, 5000 ppm CO, 1000 ppm NO, 1670 ppm H_2, 525 ppm C_2H_4, 500 ppm C_3H_6, 150 ppm C_3H_8.

3.4. Oxygenated fuel components

Many of the most promising fuel components under consideration within Co-Optima include oxygen-containing functional groups. There are two drivers behind the oxygen content: (1) biomass contains a significant amount of oxygen, which is often incorporated in bio-derived fuels; and (2) the oxygen-containing functional groups tend to impart desirable fuel properties, including resistance to engine knock (as measured by Research Octane Number) [3]. To capture the effects of oxygenated fuel components on catalyst light-off, a range of oxygen-containing compounds were included in this investigation, including alcohols, ketones, esters, and ethers.

3.4.1. Alcohols

As part of our study, we have investigated the light-off behavior of several alcohols such as ethanol, n-propanol, iso-propanol, n-butanol and iso-butanol on a hydrothermally aged commercial TWC. In Figure 5, the alcohols with equal number of carbon atoms are shown in the same color, while alcohols with a branched structure are shown in bold. This representation highlighting the structural differences between the different hydrocarbons is maintained in the figures for each functional group henceforth unless mentioned otherwise.

With the E10 surrogate fuel as the baseline, hydrocarbons which light off earlier than E10 on the aged catalyst are likely to meet the current emissions regulations with minimal modifications to the existing emissions control technology for gasoline-fueled light-duty vehicles (TWC) making them promising high-performance fuel candidates in terms of their reactivity on the TWC. Among the oxygenated hydrocarbons that we have investigated in this study, alcohols with 2 (C_2) or 3 (C_3) carbon atoms had the lowest light-off temperatures on the hydrothermally aged TWC. Alcohols with 4 carbon atoms (C_4), on the other hand, exhibited a distinct two-stage light-off profile when compared to the C_2 or C_3 alcohols as shown in Figure 5. For the same number of carbon atoms, a branched alcohol lights-off marginally earlier than a straight-chain alcohol.

Alcohols typically undergo dehydrogenation or dehydration depending on the number of carbons in the alcohols [26]. Primary and secondary alcohols with fewer carbon atoms are likely to form highly reactive aldehyde and ketone intermediates,

respectively, by hydrogen abstraction from the alcohol. We have observed the formation of acetaldehyde intermediate below 200 °C for ethanol and n-propanol and a ketone intermediate for iso-propanol. Additionally, for n-propanol, the formation of ethene was also observed between 175 to 275 °C. As alkenes are less reactive than ketones, this could explain the slower approach to full conversion with n-propanol compared to iso-propanol.

The intermediates detected during iso-butanol and n-butanol reactions shown in Figure 6 provide insights into the higher light-off temperatures of these alcohols. Both n-butanol and iso-butanol formed aldehyde intermediates (~150 °C) and alkene (C_{3+}) intermediates between 175 to 290 °C. At the onset of light-off of iso-butanol and n-butanol, iso-butyraldehyde and butyraldehyde intermediates are formed respectively. We have observed the formation of butyraldehyde for n-butanol; however, for iso-butanol, the corresponding aldehyde intermediate is probably iso-butyraldehyde [27] for which an FTIR quantification method was unavailable. In the aldehyde concentration profiles for iso-butanol and n-butanol shown in Figure 6, the first peak most likely corresponds to the dehydrogenation pathway for oxidation of alcohols resulting in the formation of aldehyde intermediates.

Once light-off of the C_4 alcohols kicks off, we observed the formation of C_{3+} alkenes. Higher number of carbon atoms in the alcohol have been found to lead to the formation of alkene intermediates by dehydration of the alcohol [26]. The C_{3+} alkenes being difficult to oxidize slow down the oxidation of the C_4 alcohols and push the light-off to higher temperatures when compared to the C_2 and C_3 alcohols. With increase in temperature, ~260 °C we observe a second aldehyde concentration feature corresponding to the onset of the alkene light-off in Figure 6 for iso-butanol as well as n-butanol. The oxidation of the aldehydes formed at the onset of the decomposition of the alkenes is likely inhibited by strongly adsorbing alkene intermediates on the active sites of the TWC leading to the interesting double-peak feature in the aldehyde concentration profiles for the C_4 alcohols. Detection of these intermediates indicate that these alcohol fuels are converted to their end products via hydrogen abstraction as well as dehydration pathways resulting in a two-stage light-off profile.

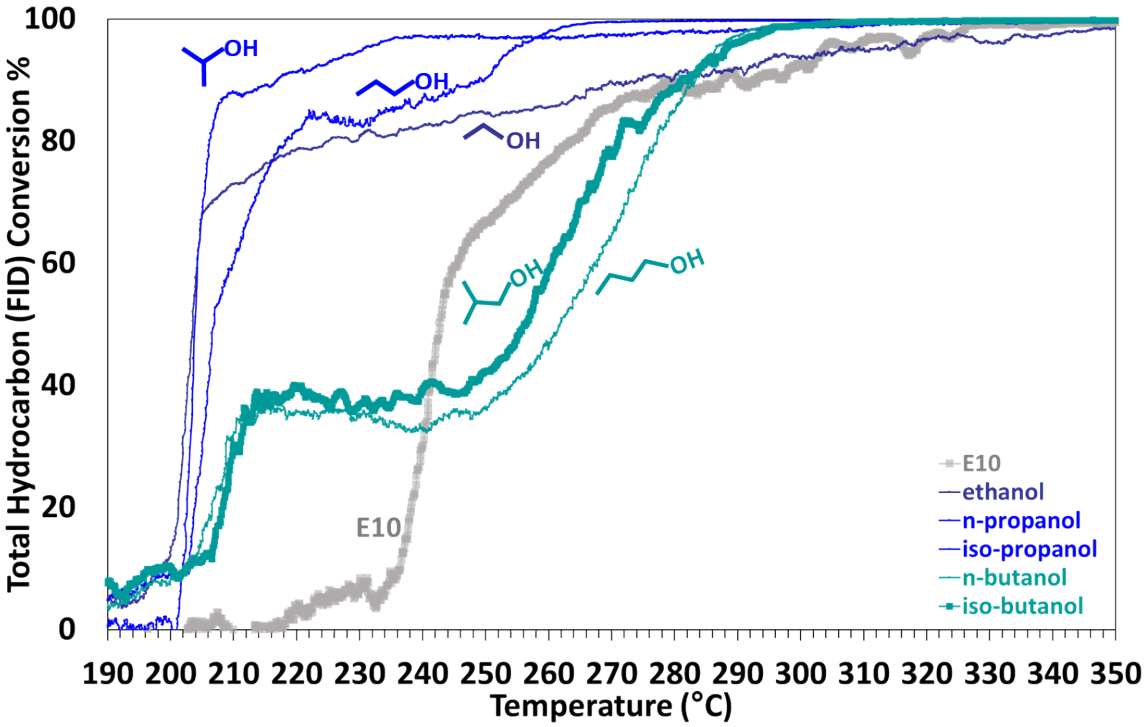

Figure 5: Comparison of total hydrocarbon conversion of straight chain and branched C_2-C_4 alcohols between catalyst inlet temperature of 100-500°C at λ = 0.999. Feed conditions: O_2, 13% CO_2, 13% H_2O, 5000 ppm CO, 1000 ppm NO, 1670 ppm H_2, 3000 ppm C_1.

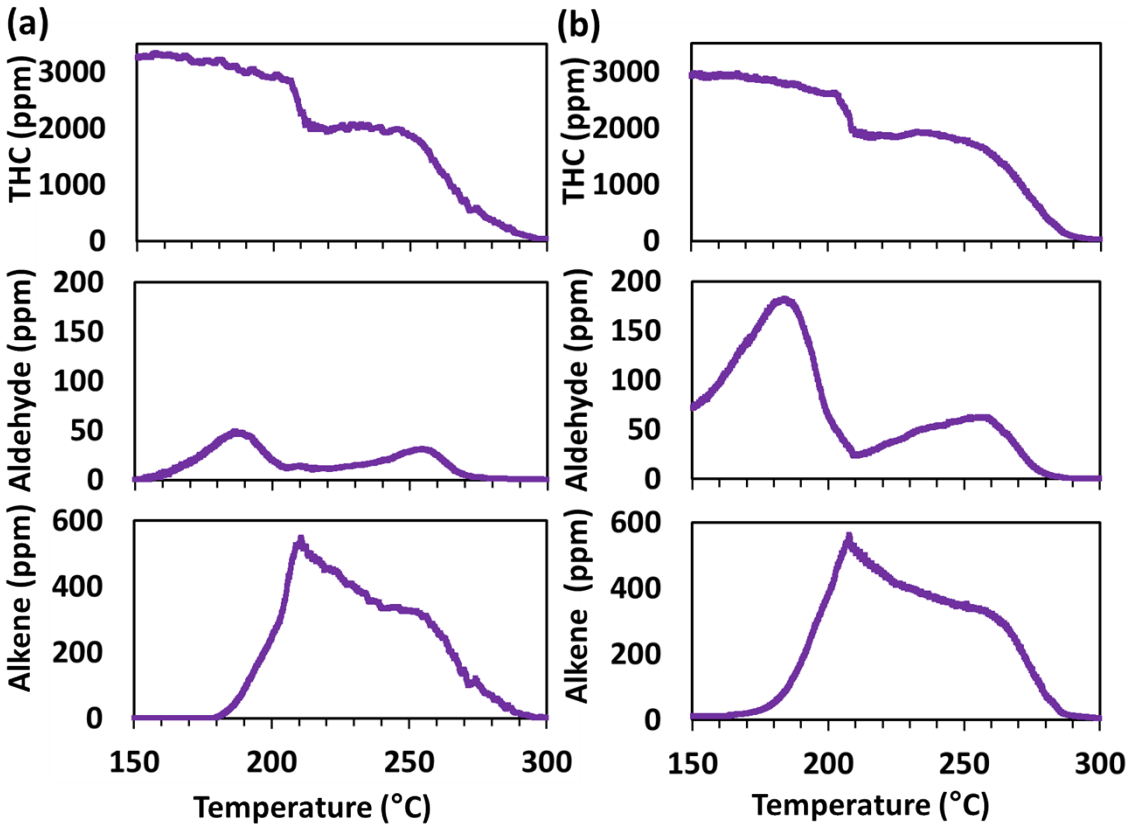

Figure 6: Total hydrocarbon (THC), aldehyde and alkene concentrations for (a) iso-butanol and (b) n-butanol between catalyst inlet temperature of 100-500°C at λ = 0.999. Feed conditions: O_2, 13% CO_2, 13% H_2O, 5000 ppm CO, 1000 ppm NO, 1670 ppm H_2, 3000 ppm C_1.

3.4.2. Ketones

As shown in Figure 7, we have investigated the reactivity of straight-chain ketones (2-butanone, 2-pentanone), a branched ketone (methyl isobutyl ketone-MIBK) and a cyclic-ketone (cyclopentanone) on a hydrothermally aged commercial TWC. For the linear ketones, an increase in the number of carbon atoms from C_4 to C_5 pushed the catalytic light-off to higher temperatures. The branched ketone, MIBK, with the higher number of carbon atoms (C_6), however, lights off earlier than the straight-chain C_5 ketone. For the same number of carbon atoms, the linear 2-pentanone lights off before the cyclic-ketone cyclopentanone. The oscillatory features observed in the case of cyclopentanone are due to vapor delivery issues as a result of swelling of the elastomers in the internal components of the vapor

delivery module rather than catalytic phenomena. With respect to the baseline E10 surrogate fuel, the linear and branched ketones were highly reactive on the TWC, while the T_{50} of the cyclic-ketone was higher than the E10 surrogate fuel.

In linear ketones such as 2-butanone and 2-pentanone, as a result of resonance with the carbonyl group (C=O), the C-H bond energies of the primary carbons (~95.5 kcal/mol) and the secondary carbons (~90.6 kcal/mol) attached to C=O are lower in comparison to the C-H bond energies further away from C=O [28,29]. Hydrogen abstraction from the secondary carbon attached to the carbonyl group, which has the lowest C-H bond energy in the ketone, is possibly where the ketone starts breaking apart. The hydrocarbon radicals thus formed then likely undergo C-C β-scission reactions resulting in complete consumption of the ketone [29,30]. Furthermore, in the case of the branched ketone, MIBK, in addition to the possible hydrogen abstraction sites mentioned for the C_4 and C_5 linear ketones, the tertiary carbon is also a likely site for hydrogen abstraction (C-H bond dissociation energy ~92.9 kcal/mol) [31].

For the cyclic-ketone, cyclopentanone, considering the axis of symmetry through C=O, the C-H bond energies are equivalent on both α-carbons (C_α- carbon to which the functional group is attached) as well as the β-carbons (C_β- carbon attached to C_α) in the molecule [32]. The presence of the C=O group weakens the C_α -H bond dissociation energies (88 kcal/mol) more than the C_β -H bond dissociation energies (~98.8 kcal/mol) [31,32]. The first step for consumption of cyclopentanone likely involves hydrogen abstraction from C_α followed by ring-opening of the resonance-stabilized radical, then radical decomposition [32,33,34]. The ring-opening step in the resonance stabilized radical likely leads to the higher light-off temperature in case of cyclopentanone.

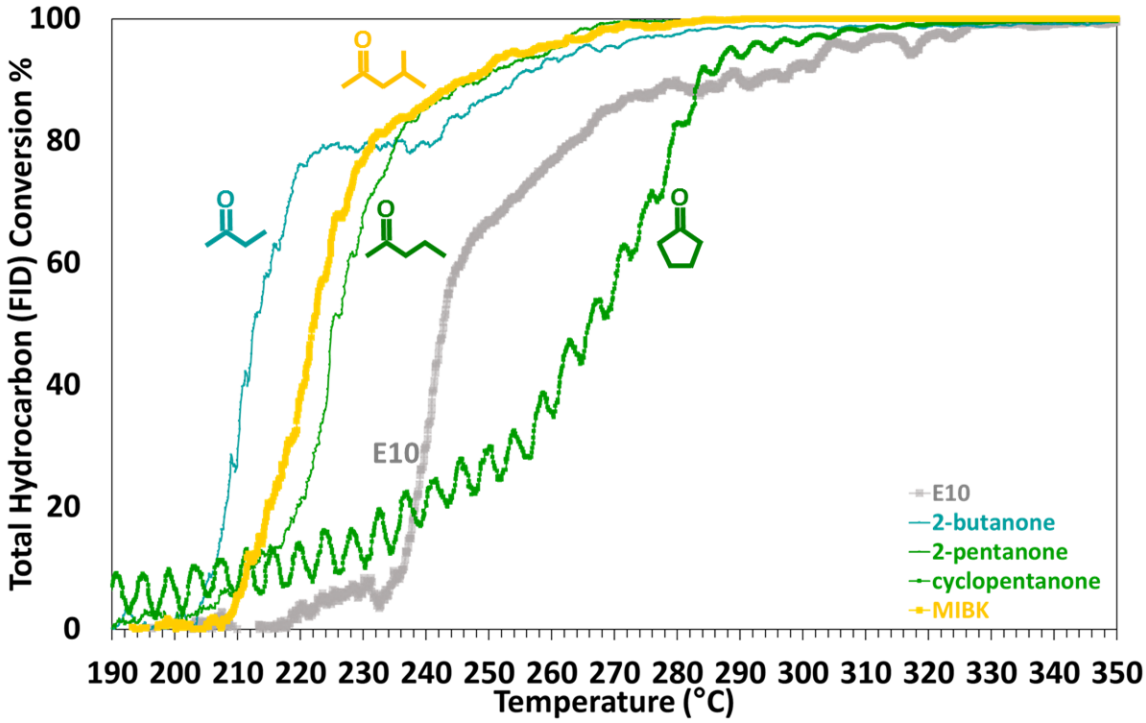

Figure 7: Comparison of total hydrocarbon conversion of straight, branched and cyclic (C_4-C_6) ketones between catalyst inlet temperature of 100-500°C at λ = 0.999. Feed conditions: O_2, 13% CO_2, 13% H_2O, 5000 ppm CO, 1000 ppm NO, 1670 ppm H_2, 3000 ppm C_1.

3.4.3. Esters

Figure 8 shows that the linear (ethyl acetate, n-butyl acetate) as well as the branched (iso-butyl acetate) alkoxy group containing esters, irrespective of the number of carbon atoms in the molecule, light off on the TWC earlier than the baseline E10 surrogate fuel. For the same number of carbon atoms, branching in the alkoxy group in the ester marginally lowers the catalytic light-off temperature of the ester.

Complete conversion of acetates into CO_2 and H_2O through alcohol/aldehyde and acetic acid pathways have been reported in the literature [14,15]. As was observed in this study, for highly active catalysts, little or no intermediates were detected. In the alkoxy section of the ester, cleavage of the O-alkyl group is favored due to its low bond dissociation energy (~91.7 kcal/mol for ethyl acetate as well as n-butyl acetate)

[31,35]. The improved reactivity of ethyl acetate, n-butyl acetate as well as iso-butyl acetate has also been attributed to the presence of β-H in the ester [36,37].

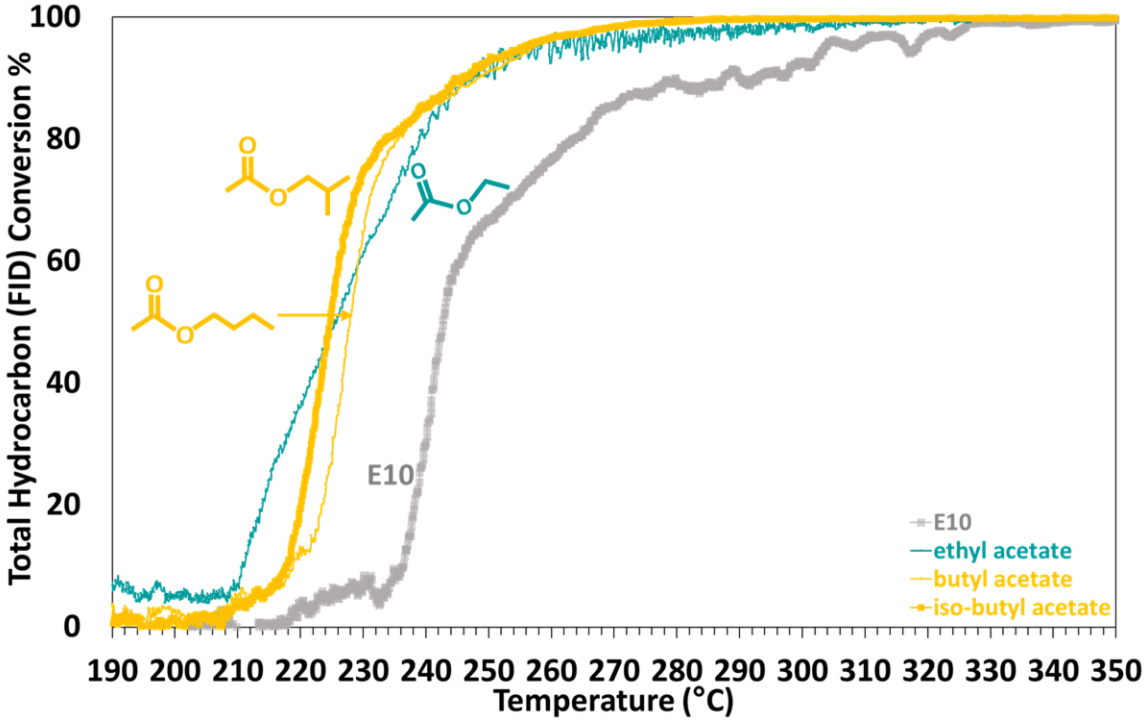

Figure 8: Comparison of total hydrocarbon conversion of straight and branched (C_4-C_6) esters between catalyst inlet temperature of 100-500°C at λ = 0.999. Feed conditions: O_2, 13% CO_2, 13% H_2O, 5000 ppm CO, 1000 ppm NO, 1670 ppm H_2, 3000 ppm C_1.

3.4.4. Aromatic Ethers

Two ether containing fuel components were included in the TWC reactivity study. The first was a mixture of of 40% 2-methylfuran and 60% 2,5-dimethylfuran, and the second was methoxybenzene (anisole). In addition to containing ether functional groups, both of these fuel candidates contain aromatic rings. Although the oxygen stability of the furans is questionable, and there are potential issues with materials compatibility with anisole, both candidates are potentially interesting fuel components due to their high RON and high energy density relative to other oxygenated compounds[3]. From Figure 9, we observe that anisole, with the 6-membered ring, has a lower T_{50} than the 5-membered furans, but both light off at higher temperatures than the E10 surrogate.

For anisole, the O-CH_3 is the weakest bond in the molecule with a bond dissociation energy of 62.9 kcal/mol followed by the C-H bond in the -OCH_3 alkoxy group (86.5 kcal/mol) [31]. The O-CH_3 bond in anisole breaks apart forming phenoxy and methyl radicals. The aromatic ring then most likely breaks down to form a resonance stabilized cyclic C_5 radical and CO. The C_5 radicals, in turn, undergo radical-radical oxidation reactions leading to the formation of open-chain C_4 radicals which then completely oxidize to form CO_2 [38,39,40].

Though they do not contain a phenyl ring, the furans are aromatic in character due to delocalization of the pi electrons from the carbon double bonds and the electrons on the oxygen atom in the ring. In the case of both components of the furan mixture tested in this study, the C-H bonds in the side alkyl groups are the weakest in their respective molecules with bond dissociation energies of 85.3 kcal/mol for 2-methylfuran and 84.8 kcal/mol for 2,5-dimethylfuran [31,41]. The higher methyl group substitution in the furan ring of 2,5-dimethylfuran makes it more reactive than 2-methylfuran. After the initial hydrogen abstraction from the methyl groups attached to the furans, resonance stabilized cyclic radicals such as 2-furanylmethyl and 5-methyl-2-furanylmethyl are formed in the case of 2-methylfuran and 2,5-dimethylfuran respectively. The inherent stability of the furan ring due to its geometric stiffness necessitates breakage of the ring before further conversion of the furan mixture is observed and likely pushes the catalytic light-off to higher temperatures. During oxidation, the furans likely undergo 5-membered ring breakage, CO elimination, and radical-radical reactions resulting in ring expansion to form phenoxy radicals or phenol [41,42,43]. Following the possible formation of phenoxy radicals, the oxidation reaction pathway leading to complete conversion of the furan mixture would closely resemble that of anisole discussed earlier.

Amongst the oxygenated fuels investigated in this study, the C_2 and C_3 alcohols, linear ketones, and esters light-off earlier than the E10 surrogate baseline fuel, while the aromatic ethers light-off later than the E10 surrogate and behave more like the non-oxygenated aromatic hydrocarbons discussed in the following section. The observed similarity in the light-off behavior between the aromatic ethers under consideration and the non-oxygenated aromatic hydrocarbons could be because the

phenoxy radical intermediates formed by the aromatic ethers follow a similar oxidation pathway to the aromatics discussed below.

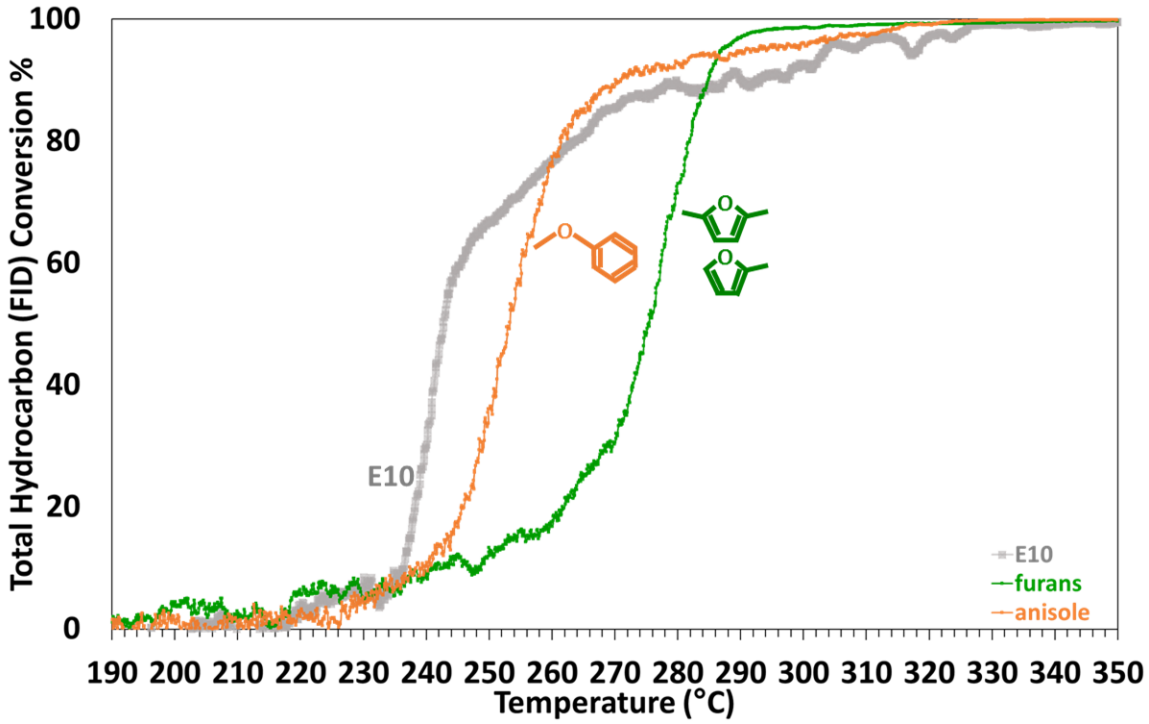

Figure 9: Comparison of total hydrocarbon conversion of aromatic ethers between catalyst inlet temperature of 100-500°C at λ = 0.999. Feed conditions: O_2, 13% CO_2, 13% H_2O, 5000 ppm CO, 1000 ppm NO, 1670 ppm H_2, 3000 ppm C_1.

3.5. Non-oxygenated hydrocarbons

While many of the promising Co-Optima blendstocks contain oxygen, there are some hydrocarbons with interesting fuel properties, including aromatics and branched alkenes. As all of the other Co-Optima blendstocks, these potential fuel components could be derived from biomass. Furthermore, the petroleum-based refinery streams into which the Co-Optima blendstocks would be mixed consist of a wide range of non-oxygenated hydrocarbons. Thus, this study included a number of different hydrocarbons, including aromatics, alkenes, linear alkanes, branched alkanes, and cycloalkanes.

3.5.1. Aromatic hydrocarbons

Aromatics have favorable fuel properties, including resistance to knocking, which is why most gasoline on the market contains approximately one quarter to one third aromatic species. Furthermore, aromatic species can be produced from biomass through multiple pathways. Thus, this investigation included toluene, m-xylene and mesitylene. In Figure 10 we observe that the three non-oxygenated aromatic fuels evaluated in this study light off after the E10 surrogate baseline on the TWC. Moreover, the T_{50} and T_{90} for toluene is lower than m-xylene, which, in turn, is lower than that of mesitylene. Increasing the methyl group substitution in the aromatic ring, therefore, pushes the fuel light off on the catalyst to higher temperatures.

The initiation of oxidation of the methyl-substituted benzene molecules is likely via hydrogen abstraction from a side methyl group as the C-H bond dissociation energy is the lowest in the methyl groups attached to the aromatic ring (~89.7 kcal/mol). For the fuels under consideration, the degree of methyl substitution in the aromatic ring does not significantly vary the C-H bond dissociation energy in the methyl groups [31,44]. However, the steric effects due to the symmetry in the distribution of the methyl groups in mesitylene may render that fuel slightly less reactive when compared to toluene and m-xylene [45].

Furthermore, the inductive effect of the methyl groups on the aromatic ring lowers the ionization potential of the hydrocarbon molecule when compared to that of unsubstituted benzene (9.24 eV). Increasing the methyl substitution in the aromatic ring further lowers the ionization potential of the hydrocarbon. Specifically, the ionization potential of toluene (8.82 eV) > m-xylene (8.56 eV) > mesitylene (8.39 eV) [46]. Lower ionization potential implies that, on catalytic activation of the molecule, the methyl-substituted hydrocarbons are likely to adsorb strongly onto the surface of the catalyst through the formation of very stable π-complexes [12,47]. Thus, higher degrees of methyl substitution in the aromatic ring result in the formation of strongly adsorbing stable intermediate species on the surface of the catalyst which possibly lead to the higher light-off temperatures observed on the TWC.

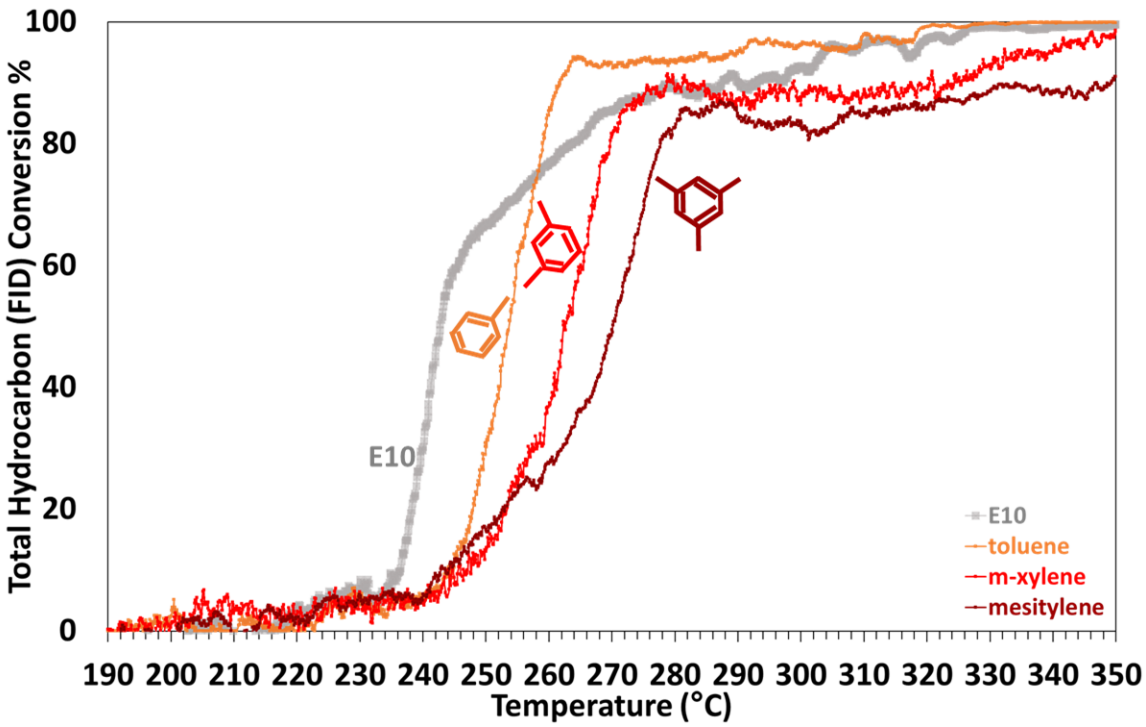

Figure 10: Comparison of total hydrocarbon conversion of aromatic hydrocarbons (C_7-C_9) between catalyst inlet temperature of 100-500°C at λ = 0.999. Feed conditions: O_2, 13% CO_2, 13% H_2O, 5000 ppm CO, 1000 ppm NO, 1670 ppm H_2, 3000 ppm C_1.

3.5.2. Alkenes

A variety of different alkenes can be found in engine exhaust, and they can come from several different sources. Small chain alkenes, such as propene and ethene, are formed through cracking and partial oxidation of fuel species in the combustion cylinder. Longer chain linear alkenes, such as 1-hexene and 1-octene, are found in conventional petroleum-derived gasoline blends. Finally, di-isobutylene, a mix of two highly branched alkenes, is one of the promising Co-Optima blendstocks. All of these alkenes were included in this investigation. From Figure 11 we observe that alkene reactivity on the TWC is sensitive to the number of carbon atoms in the molecule. The C_2 alkene, ethene, lights off earlier than the E10 surrogate baseline fuel while

the C_3-C_8 linear alkenes light-off after E10 surrogate. Increasing the number of carbon atoms in the linear alkenes shifts the catalyst light-off to higher temperatures. Additionally, for the same number of carbon atoms in the molecule (C_8), the branched alkene, diisobutylene, was found to be more reactive on the TWC under synthetic exhaust flow conditions compared to the linear alkene, 1-octene.

Although the vinylic H atoms in ethene have high C-H bond dissociation energies (110.9 kcal/mol), in Figure 11 we observe that ethene lights off the earliest amongst the alkenes in this study. This is possibly due to ethene interacting with the catalyst surface primarily through its π-bond rather than molecule activation through hydrogen abstraction from ethene. The transformation of the π-bond into di-σ bonds is favored as the former type of interaction with the surface of the catalyst is more sensitive to steric effects and is known to resist rehybridization of the molecule which is an important step in the oxidation process [31,48,49,50]. The high ionization potential of ethene (10.51 eV) indicates that the intermediate radicals formed possibly undergo addition reactions with oxygenated radicals and readily desorb from the catalyst surface [51].

Allylic hydrogen atoms in C_3 and longer alkenes are more reactive than the vinylic H atoms on alkenes due to their lower C-H bond dissociation energy, especially when the hydrogen is attached to a secondary carbon atom [52]. The allylic H is connected to a primary C atom in propene which elevates the C-H bond dissociation energy to 88.2 kcal/mol, whereas, for 1-hexene and 1-octene, the C-H bond dissociation energy is 83.4 kcal/mol since the allylic H atom is bonded to a secondary carbon atom. The presence of these allylic H atoms, therefore, make hydrogen abstraction from these sites favorable for the C_3, C_6 and C_8 alkenes. Furthermore, longer alkyl chains result in weaker C-C bonds between the alkyl-allyl groups after allyl radical formation, as exemplified by the C-C bond dissociation energies between the alkyl-allyl group in 1-hexene (75 kcal/mol) and 1-octene (73.3 kcal/mol) [31]. Competition between addition reactions and abstraction mechanisms have been reported for the longer chain alkenes [53,54].

On abstraction of the allylic hydrogen in propene, 1-hexene, 1-octene and diisobutylene, resonance stabilized π-complexes are formed. For the linear alkenes,

with increase in the number of carbons in the α-olefin, the ionization potential decreases implying higher stability of its π-complex due to electron delocalization [51]. Therefore, on the TWC, we observe that as the number of carbon atoms in the linear alkene increases, the catalytic light-off is pushed to higher temperatures. Moreover, for a branched alkene such as diisobutylene, the presence of two methyl groups on the same C atom has a destabilizing effect on the π-complex [51], which could provide a possible explanation for the earlier catalytic light-off of the branched C_8 alkene than the linear C_8 alkene.

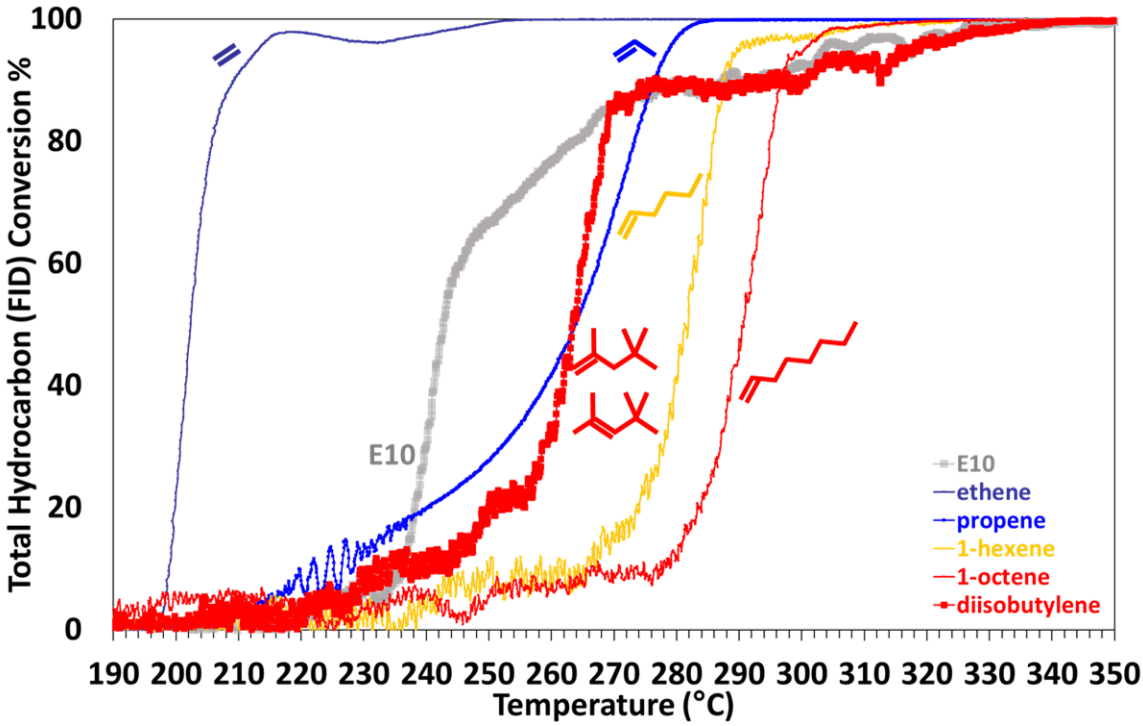

Figure 11: Comparison of total hydrocarbon conversion of straight and branched alkenes (C_2-C_8) between catalyst inlet temperature of 100-500°C at λ = 0.999. Feed conditions: O_2, 13% CO_2, 13% H_2O, 5000 ppm CO, 1000 ppm NO, 1670 ppm H_2, 3000 ppm C_1.

3.5.3. Alkanes

The impact of hydrocarbon structure on its reactivity on the TWC under synthetic exhaust flow conditions is further pronounced in the case of alkanes. As mentioned above, gasoline contains a wide range of alkanes, including linear alkanes such as n-heptane (C_7) and n-octane (C_8); branched alkanes such as 2-methylpentane (C_6)

and iso-octane (C_8); and cycloalkanes such as methylcyclopentane (C_6) and methylcyclohexane (C_7); all of these species were included in this study. Also, since they are widely used as fuels in SI engines, and because they represent the lower limit for short chain alkanes, methane and propane were also included. From Figure 12, which depicts the light-off behavior of the various alkanes considered in this study, several interesting trends associated with the structure of the alkanes emerge. Firstly, we observe that in the case of linear alkanes, short-chain methane and propane fuels light-off on the TWC at much higher temperatures (> 300 ºC) than the longer linear alkanes such as n-heptane and n-octane. Increasing in the number of carbon atoms in a linear alkane increases the reactivity of the alkane molecule on the TWC. Methane is particularly unreactive, and does not reach 90% conversion (T_{90}) in the temperature range that we have considered in this study. Secondly, the shape of the light-off curves of the branched alkanes, 2-methylpentane and iso-octane, while being similar to each other, are distinct from the other alkanes evaluated in this study. Furthermore, for the same number of carbon atoms in the hydrocarbon molecule (C_8), the linear alkane, n-octane, is more reactive on the TWC compared to the branched alkane, iso-octane. In the case of the cycloalkanes, the catalytic light-off temperature of methylcyclohexane is lower than that of methylcyclopentane. With the E10 surrogate fuel as reference, Figure 12 demonstrates that the long-chain alkanes and cycloalkanes light off earlier than E10 while the branched alkanes and the short-chain light alkanes light off after E10. Overall, the following trend of the catalytic reactivity on the TWC for the alkanes is revealed: long-chain n-alkanes > cycloalkanes > E10 surrogate > branched alkanes > short-chain alkanes.

Activation of alkanes on the catalyst surface by abstraction of the weakest C-H bond in the saturated hydrocarbon has been widely reported [18,20,23,55]. Methane is particularly stable with the highest C-H bond dissociation energy among the alkanes (105 kcal/mol) and lights off on the catalyst the latest among all the fuels tested in this study. In propane, hydrogen is likely abstracted from the secondary C atom (98.1 kcal/mol) rather than that attached to the primary C atom (101 kcal/mol). In the longer linear alkanes (C_7, C_8), the secondary C-H bonds connected to the terminal

methyl groups are the weakest in the molecule (98 kcal/mol) and are likely to undergo hydrogen abstraction. The methyl-substituted cycloalkanes are possibly activated by hydrogen abstraction from the attached methyl group (93.7-94.3 kcal/mol). The oxidation mechanism of the cycloalkanes has been likened to that of acyclic alkanes once the ring opens [56,57]. The ease of formation of the reactive 6-membered intermediate in the case of methylcyclohexane compared to methylcyclopentane possibly enhances its reactivity on the TWC.

In the branched alkanes, 2-methylpentane and iso-octane, the H atom associated with the tertiary C atom likely undergoes H-abstraction as they have the lowest bond dissociation energies in their respective molecules at 94.7 kcal/mol and 95.6 kcal/mol respectively [31]. However, for these branched alkanes, with increase in substitution at the C atom vicinal to the terminal methyl group, further reaction involving C-C bond cleavage of the alkyl radical formed is delayed until additional hydrogen abstractions from the molecule weaken the bond [58]. Increase in the number of carbons in the linear alkane favors the formation of highly reactive peroxyalkyl intermediates resulting in complete consumption of the fuel molecule. Branching in the alkane, however, likely forms less reactive alkene or cyclic-ether intermediates, thus pushing the catalytic light-off to higher temperatures [56].

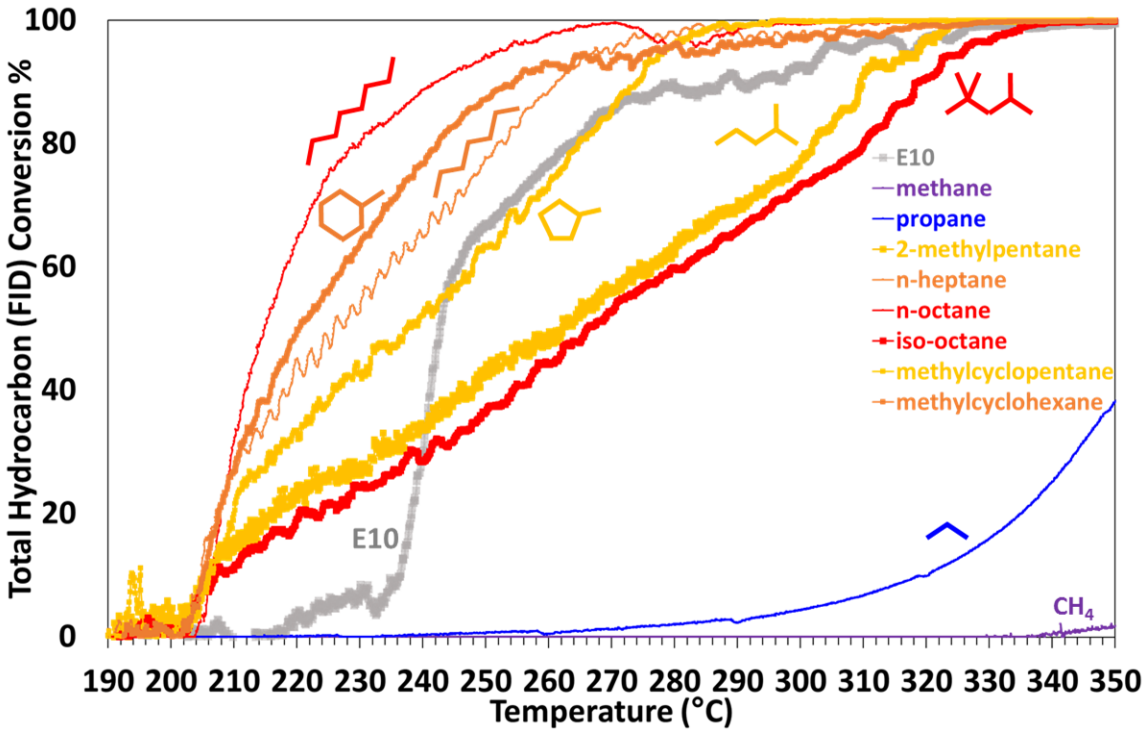

Figure 12: Comparison of total hydrocarbon conversion of straight, branched and cyclic alkanes (C_1-C_8) between catalyst inlet temperature of 100-500°C at λ = 0.999. Feed conditions: O_2, 13% CO_2, 13% H_2O, 5000 ppm CO, 1000 ppm NO, 1670 ppm H_2, 3000 ppm C_1.

3.5.4. Comparison across non-oxygenated hydrocarbons

The sensitivity of the catalytic reactivity of the non-oxygenated hydrocarbons to their structure is highlighted in Figures 13 and 14 in which the stark differences in hydrocarbon light-off behaviors and the corresponding CO conversion on the TWC for all of the evaluated C_8 fuel components are depicted. Figure 13 reveals very different trends in alkane and alkene reactivities on the TWC under synthetic engine exhaust conditions. The linear alkane, n-octane, lights off much earlier than the linear alkene, 1-octene; in fact, it was one of the most reactive species evaluated here. The formation of strongly adsorbing resonance stabilized radicals on the surface of the catalyst in the case of the linear alkene would explain the vast differences in the light-off temperatures between the two linear C_8 fuels. Furthermore, branching has opposite effects in alkanes and alkenes. In the C_8 alkane, branching pushes the light-off to higher temperatures due to the presence of the stable quaternary carbon atom in the molecule, while a branched C_8 alkene is

more reactive than its linear counterpart as increased methyl-substitution destabilizes the intermediate π-complex formed on the catalyst surface [20,23]. The impact of the structure of the fuel and its reactivity on the TWC is further pronounced when observing the CO conversion shown in Figure 14. While the C_8 alkanes have minimal effects on the CO light-off, the C_8 alkenes and m-xylene significantly deter CO activity, indicating the inhibitive effect of the intermediates formed in the latter cases. These distinctive results based on the nature of the fuel structure emphasize the importance of evaluating the effect of hydrocarbon light-off on other regulated pollutants such as CO and NO_x, as is discussed in the following section.

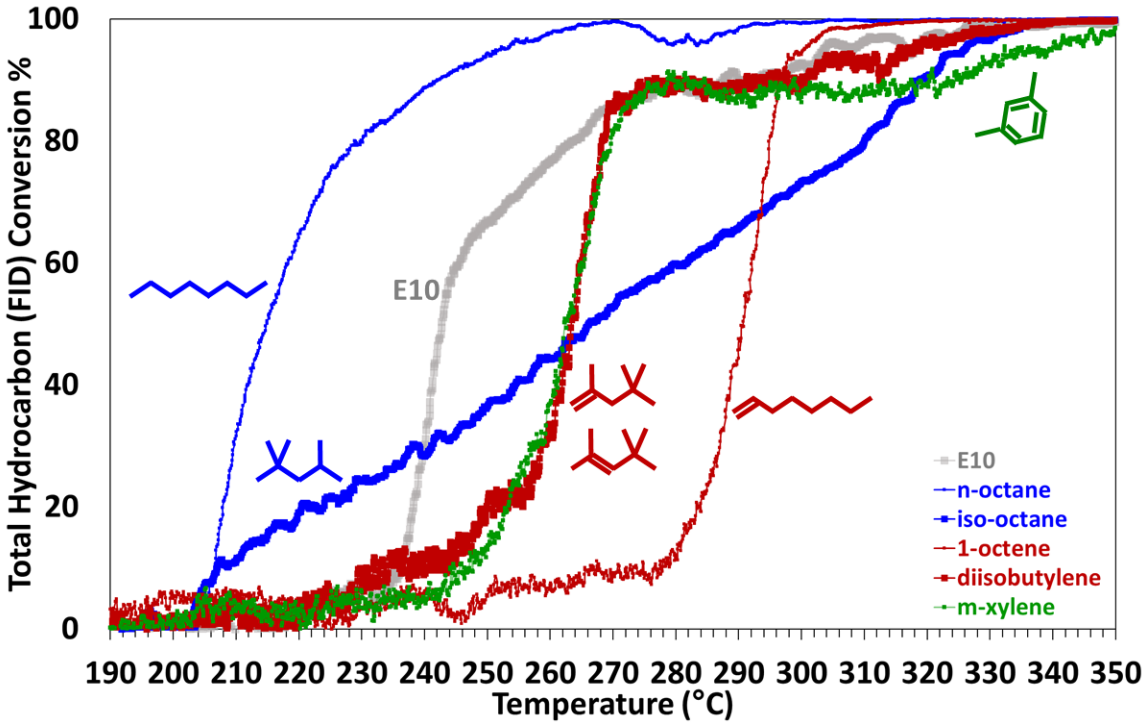

Figure 13: Comparison of total hydrocarbon conversion of C_8 fuels between catalyst inlet temperature of 100-500°C at λ = 0.999. Feed conditions: O_2, 13% CO_2, 13% H_2O, 5000 ppm CO, 1000 ppm NO, 1670 ppm H_2, 3000 ppm C_1.

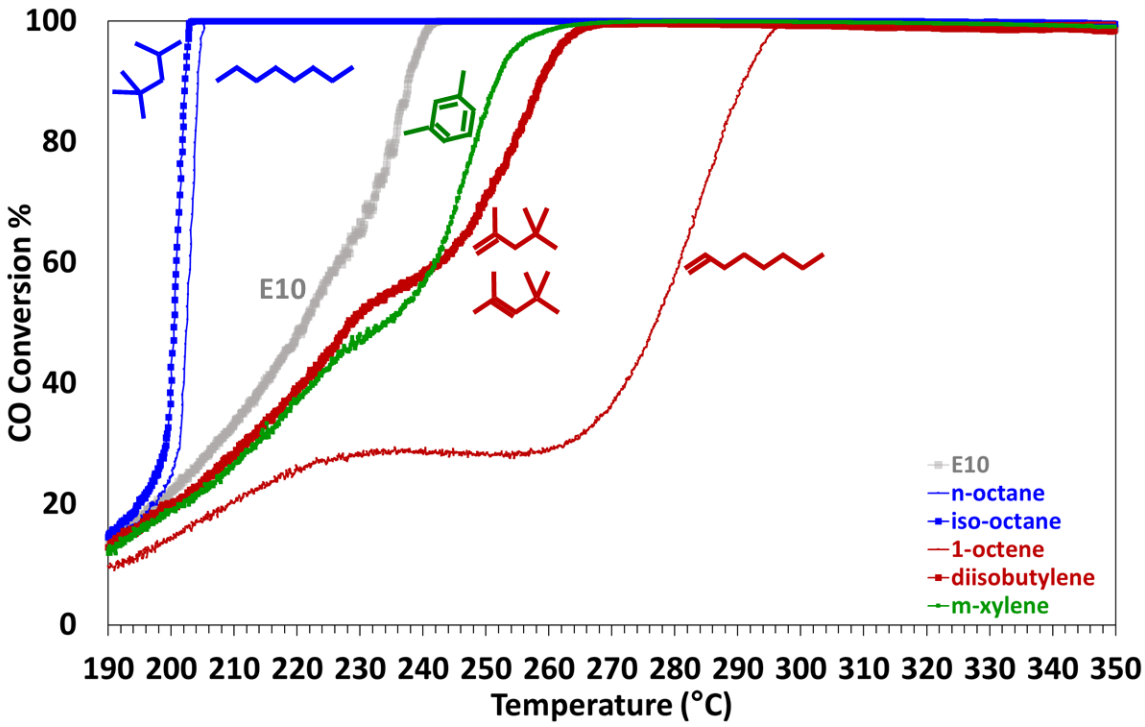

Figure 14: Comparison of CO conversion of C_8 fuels between catalyst inlet temperature of 100-500°C at λ = 0.999. Feed conditions: O_2, 13% CO_2, 13% H_2O, 5000 ppm CO, 1000 ppm NO, 1670 ppm H_2, 3000 ppm C_1.

3.6. Effect of hydrocarbon light-off on other regulated pollutants

3.6.1. Nitrogen oxides (NO_x) light-off

A summary of the reactivities of the hydrocarbons on the TWC under synthetic engine exhaust conditions is captured by the comparison of the T_{50} and T_{90}s of the fuels shown in Figure 15 (a). Overall, we observe the following trend in light-off temperatures: C_2 and C_3 alcohols < linear ketones, branched ketones < long-chain alkanes < esters, cycloalkanes < E10 surrogate < aromatic ethers, aromatic hydrocarbons < alkenes < short-chain alkanes. The impact of the specific hydrocarbon light-off on the NO_x T_{50}s and T_{90}s is displayed in Figure 15 (b). We observe that, irrespective of the type of fuel, the NO_x T_{50}s are comparable over the range of fuels tested. At low temperatures, NO_x species react with CO and H_2 in the feed and are reduced over the TWC. As the synthetic exhaust flow reactor is operated at close to stoichiometric conditions (λ = 0.999), and there is a significant

concentration of hydrocarbons in the gas mixture, there is insufficient CO and H_2 to convert all of the NOx. Complete NOx conversion requires nearly all of the hydrocarbons to react. This is why the NO_x T_{90}s track the HC T_{90} trends observed for the respective fuels shown in Figure 15 (a). Critically, this result shows that reactivity of the exhaust HCs over the TWC impacts not just NMOG emissions, but NOx emissions as well.

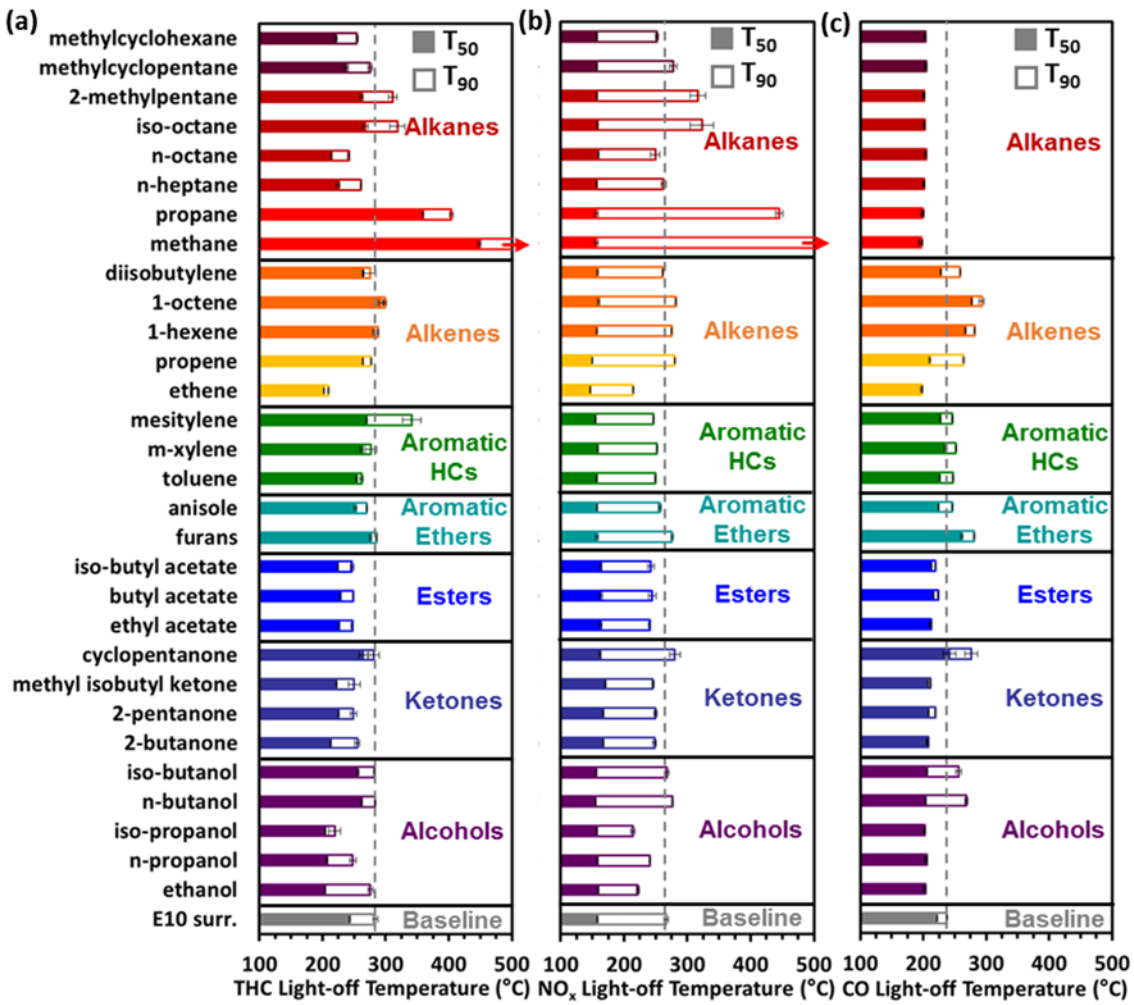

Figure 15: Comparison of T_{50} and T_{90} of the (a) hydrocarbons (THC) and its effect on (b) NO_x and (c) CO light-off temperatures. Feed conditions: O_2, 13% CO_2, 13% H_2O, 5000 ppm CO, 1000 ppm NO, 1670 ppm H_2, 3000 ppm C_1, λ = 0.999.

3.6.2. Carbon monoxide (CO) light-off

The effect of catalytic light-off of the hydrocarbons on CO conversions is displayed in Figure 15 (c). As discussed above, the fuel components under consideration fall under two distinct categories: those that inhibit CO oxidation, and those that do not. For the non-inhibiting species, the CO light-off occurs at around 200 °C, and the light-off profile is nearly vertical, resulting in T_{50}s an T_{90}s that are essentially the same. The non-inhibiting species include alkanes, esters, linear and branched ketones, and C_2 and C_3 alcohols. Note that the HC light-off for these species varies widely, but the CO oxidation behavior is essentially the same, supporting indicating that these species do not block the CO oxidation sites on the catalyst, and therefore there is no correlation between HC and CO conversion. The inhibiting species, on the other hand, result in both higher light-off temperatures and a more gradual light-off process, as seen in the differences between T_{50} and T_{90}. The inhibiting species include alkenes, aromatic hydrocarbons, aromatic ethers, the cycloketone, and C_4 alcohols. Comparing the CO T90s in Figure 15 (c) to the HC T90s in Figure 15 (a) for the inhibiting species, there is a fairly strong correlation between complete conversion of CO and complete conversion of HCs, indicating that the HCs must be fully converted before CO is completely oxidized. This is consistent with inhibiting fuel species blocking the CO oxidation active sites.

4. Conclusion

Considering E10 surrogate (65% iso-octane, 25% toluene, 10% ethanol) as the baseline (λ=0.999), fuels that light-off on the hydrothermally aged three-way catalyst (TWC) earlier than the E10 surrogate fuel are promising high-performance fuel candidates in terms of their reactivity on existing emission control technology (TWC) and are likely to meet the current emissions regulations with minimal modifications to existing exhaust aftertreatment architectures. The light-off behaviors of the fuels under consideration were found to be highly variable depending on the functional group the specific hydrocarbon belonged to:

- The oxygenated hydrocarbons other than aromatic ethers and cyclo-ketone demonstrated higher reactivity on the TWC than the baseline fuel as well as the non-oxygenated fuels.
- The non-oxygenated hydrocarbons, especially, exhibited interesting structure-reactivity trends.
    - With increase in methyl substitution in the aromatic ring of the non-oxygenated aromatic hydrocarbons, the light-off temperature increased.
    - Opposing trends were observed in the case of alkanes and alkenes: in the case of linear alkanes, increase in the number of carbon atoms in the molecule resulted in lower light-off temperatures on the TWC while in the case of linear alkenes, increase in chain length pushed catalytic light-off to higher temperatures.
    - For the same number of carbon atoms in the hydrocarbon, a branched alkane was found to be less reactive than a linear alkane whereas a branched alkene demonstrated higher reactivity on the TWC than a linear alkene.
- Overall, in terms of reactivity on the TWC: C_2, C_3 alcohols > long-chain linear alkanes, branched ketones > esters, cycloalkanes > E10 surrogate baseline > aromatic ethers aromatic hydrocarbons > alkenes > short-chain alkanes.
- Depending on the type of fuel, the catalytic light-off of other regulated pollutants such as CO and NO_x (nitrogen oxides) were also impacted.

- In the case of CO light-off, the fuels either had a non-inhibiting (alkanes, esters, linear and branched ketones, C_2 and C_3 alcohols) or an inhibiting effect (alkenes, aromatic hydrocarbons, aromatic ethers, cycloketone and C_4 alcohols).
- In the case of NOx light-off, while the T_{50}s were comparable for all the fuels considered in this study, the T_{90}s were achieved once the hydrocarbons were completely oxidized.

The catalytic light-off measurements of individual fuel components on a commercial TWC emphasizes the importance of evaluating more realistic hydrocarbons rather than model hydrocarbons such as propene to accurately capture fuel-composition effects on emissions of regulated pollutants. Additionally, the individual fuel light-off profiles can be used as a foundation for predicting the catalytic light-off behavior of multi-component fuel blends representative of real-world fuels.

5. Acknowledgement

This report and the work described were sponsored by the U.S. Department of Energy (DOE) Bioenergy Technologies Office (BETO) and Vehicle Technologies Office (VTO) under the DOE Co-Optimization of Fuels and Engines Initiative. The authors gratefully acknowledge the support and direction of Kevin Stork at VTO, Alicia Lindauer at BETO, and the Co-Optima Leadership Team.

6. References

(1) Szybist, J. P.; Splitter, D. A. Understanding Chemistry-Specific Fuel Differences at a Constant RON in a Boosted SI Engine. **2018**, *217* (January), 370–381. https://doi.org/10.1016/j.fuel.2017.12.100.

(2) Kalghatgi, G. T. Fuel Anti-Knock Quality - Part I . Engine Studies. *SAE Int.* **2018**, No. 2001-01–3584. https://doi.org/10.4271/2001-01-3584.

(3) McCormick, R. L.; Fioroni, G.; Fouts, L.; Christensen, E.; Yanowitz, J.; Polikarpov, E.; Albrecht, K.; Gaspar, D. J.; Gladden, J.; George, A. Selection Criteria and Screening of Potential Biomass-Derived Streams as Fuel Blendstocks for Advanced Spark-Ignition Engines. *SAE Int. J. Fuels Lubr.* **2017**, *10* (2), 2017-01–0868. https://doi.org/10.4271/2017-01-0868.

(4) *Rules and Regulations, 79 Federal Register 81*; 2014.

(5) Wang, J.; Chen, H.; Hu, Z.; Yao, M.; Li, Y. A Review on the Pd-Based Three-Way Catalyst. *Catal. Rev. - Sci. Eng.* **2015**, *57* (1), 79–144. https://doi.org/10.1080/01614940.2014.977059.

(6) Bäroth, T.; Drochner, A.; Vogel, H.; Votsmeier, M. Effect of Diverse Hydrocarbons on the Cold Start Behavior of Three-Way Catalysts. *Top. Catal.* **2017**. https://doi.org/10.1007/s11244-016-0609-8.
(7) Reiter, M. S.; Kockelman, K. M. The Problem of Cold Starts: A Closer Look at Mobile Source Emissions Levels. *Transp. Res. Part D Transp. Environ.* **2016**, *43* (x), 123–132. https://doi.org/10.1016/j.trd.2015.12.012.
(8) Patterson, M. J.; Angove, D. E.; Cant, N. W. The Effect of Carbon Monoxide on the Oxidation of Four C6 to C8 Hydrocarbons over Platinum, Palladium and Rhodium. *Appl. Catal. B Environ.* **2000**. https://doi.org/10.1016/S0926-3373(00)00110-7.
(9) Pontikakis, G. N.; Konstantas, G. S.; Stamatelos, A. M. Three-Way Catalytic Converter Modeling as a Modern Engineering Design Tool. *J. Eng. Gas Turbines Power* **2004**, *126* (4), 906. https://doi.org/10.1115/1.1787506.
(10) Heo, I.; Choung, J. W.; Kim, P. S.; Nam, I. S.; Song, Y. Il; In, C. B.; Yeo, G. K. The Alteration of the Performance of Field-Aged Pd-Based TWCs towards CO and C3H6 Oxidation. *Appl. Catal. B Environ.* **2009**, *92* (1–2), 114–125. https://doi.org/10.1016/j.apcatb.2009.07.016.
(11) Becker, L.; Förster, H. Oxidative Decomposition of Benzene and Its Methyl Derivatives Catalyzed by Copper and Palladium Ion-Exchanged Y-Type Zeolites. *Appl. Catal. B Environ.* **1998**, *17* (1–2), 43–49. https://doi.org/10.1016/S0926-3373(97)00102-1.
(12) Ordóñez, S.; Bello, L.; Sastre, H.; Rosal, R.; Díez, F. V. Kinetics of the Deep Oxidation of Benzene, Toluene, N-Hexane and Their Binary Mixtures over a Platinum on γ-Alumina Catalyst. *Appl. Catal. B Environ.* **2002**, *38* (2), 139–149. https://doi.org/10.1016/S0926-3373(02)00036-X.
(13) Shim, W. G.; Jung, S. C.; Seo, S. G.; Kim, S. C. Evaluation of Regeneration of Spent Three-Way Catalysts for Catalytic Oxidation of Aromatic Hydrocarbons. *Catal. Today* **2011**, *164* (1), 500–506. https://doi.org/10.1016/j.cattod.2010.10.039.
(14) Larsson, P. O.; Andersson, A. Complete Oxidation of CO, Ethanol, and Ethyl Acetate over Copper Oxide Supported on Titania and Ceria Modified Titania. *J. Catal.* **1998**, *179* (1), 72–89. https://doi.org/10.1006/jcat.1998.2198.
(15) Musialik-Piotrowska, A.; Syczewska, K. Combustion of Volatile Organic Compounds in Two-Component Mixtures over Monolithic Perovskite Catalysts. *Catal. Today* **2000**, *59* (3), 269–278. https://doi.org/10.1016/S0920-5861(00)00293-5.
(16) Assebban, M.; Kasmi, A. El; Harti, S.; Chafik, T. Intrinsic Catalytic Properties of Extruded Clay Honeycomb Monolith Towardscomplete Oxidation of Air Pollutants. *J. Hazard. Mater. jo* **2015**, *300*, 590–597. https://doi.org/10.1016/j.jhazmat.2015.07.067.
(17) Matějová, L.; Topka, P.; Jirátová, K.; Šolcová, O. Total Oxidation of Model Volatile Organic Compounds over Some Commercial Catalysts. *Appl. Catal. A Gen.* **2012**, *443–444*, 40–49. https://doi.org/10.1016/j.apcata.2012.07.018.
(18) Burch, R.; Crittle, D. J.; Hayes, M. J. C–H Bond Activation in Hydrocarbon Oxidation on Heterogeneous Catalysts. *Catal. Today* **1999**, *47* (1–4), 229–234. https://doi.org/10.1016/S0920-5861(98)00303-4.

(19) O'Malley, A.; Hodnett, B. K. The Influence of Volatile Organic Compound Structure on Conditions Required for Total Oxidation. *Catal. Today* **1999**, *54* (1), 31–38. https://doi.org/10.1016/S0920-5861(99)00166-2.
(20) Diehl, F.; Barbier, J.; Duprez, D.; Guibard, I.; Mabilon, G. Catalytic Oxidation of Heavy Hydrocarbons over Pt/Al2O3. Influence of the Structure of the Molecule on Its Reactivity. *Appl. Catal. B Environ.* **2010**. https://doi.org/10.1016/j.apcatb.2009.12.026.
(21) McCabe, R. W.; Siegl, W. O.; Chun, W.; Jr, J. P. Speciated Hydrocarbon Emissions from the Combustion of Single Component Fuels . II . Catalyst Effects Speciated Hydrocarbon Emissions from the Combustion of Single Component Fuels . II . Catalyst Effects. **2013**, *3289* (March), 37–41. https://doi.org/10.1080/10473289.1992.10467054.
(22) Poulopoulos, S. G.; Samaras, D. P.; Philippopoulos, C. J. Regulated and Speciated Hydrocarbon Emissions from a Catalyst Equipped Internal Combustion Engine. *Atmos. Environ.* **2001**, *35* (26), 4443–4450. https://doi.org/10.1016/S1352-2310(01)00231-X.
(23) Kang, S. B.; Nam, S. B.; Cho, B. K.; Nam, I. S.; Kim, C. H.; Oh, S. H. Effect of Speciated HCs on the Performance of Modern Commercial TWCs. *Catal. Today* **2014**, *231*, 3–14. https://doi.org/10.1016/j.cattod.2013.11.032.
(24) *Aftertreatment Protocols for Catalyst Characterization and Performance Evaluation: Low-Temperature Oxidation Catalyst Test Protocol*; 2015.
(25) Pihl, J. A.; Toops, T. J.; Fisher, G. B.; West, B. H. Selective Catalytic Reduction of Nitric Oxide with Ethanol/gasoline Blends over a Silver/alumina Catalyst. *Catal. Today* **2014**, *231*, 46–55.
(26) Norton, T. S.; Dryer, F. L. The Flow Reactor Oxidation of C1-C4 Alcohols and MTBE. *Symp. Combust.* **1991**. https://doi.org/10.1016/S0082-0784(06)80257-2.
(27) Brookshear, D. W.; Pihl, J. A.; Toops, T. J.; West, B.; Prikhodko, V. The Selective Catalytic Reduction of NOx over Ag/Al2O3 with Isobutanol as the Reductant. *Catal. Today* **2016**, *267* (x), 65–75. https://doi.org/10.1016/j.cattod.2016.01.034.
(28) Hudzik, J. M.; Bozzelli, J. W. Thermochemistry and Bond Dissociation Energies of Ketones. *J. Phys. Chem. A* **2012**, *116* (23), 5707–5722. https://doi.org/10.1021/jp302830c.
(29) Minwegen, H.; Burke, U.; Heufer, K. A. An Experimental and Theoretical Comparison of C3-C5 Linear Ketones. *Proc. Combust. Inst.* **2017**, *36* (1), 561–568. https://doi.org/10.1016/j.proci.2016.05.050.
(30) Hemken, C.; Burke, U.; Graf, I.; Ruwe, L.; Park, S.; Sarathy, S. M.; Heufer, K. A.; Kohse-Höinghaus, K. A Laminar Flame Investigation of 2-Butanone, and the Combustion-Related Intermediates Formed through Its Oxidation. *Proc. Combust. Inst.* **2017**, *36* (1), 1175–1183. https://doi.org/10.1016/j.proci.2016.06.082.
(31) Luo, Y.-R. *Comprehensive Handbook of Chemical Bond Enegies*; CRC Press, 2007.
(32) Thion, S.; Togbé, C.; Dayma, G.; Serinyel, Z.; Dagaut, P. Experimental and Detailed Kinetic Modeling Study of Cyclopentanone Oxidation in a Jet-Stirred Reactor at 1 and 10 Atm. *Energy & Fuels* **2017**, *31* (3), 2144–2155. https://doi.org/10.1021/acs.energyfuels.6b02061.
(33) Zaras, A. M.; Thion, S.; Dagaut, P. Computational Kinetic Study for the

Unimolecular Decomposition of Cyclopentanone. *Int. J. Chem. Kinet.* **2015**, *47* (7), 439–446. https://doi.org/10.1002/kin.20921.
(34) Delles, F. M.; Dodd, L. T.; Lowden, L. F.; Romano, F. J.; Daignault, L. G. The Pyrolysis of Cyclopentanone. *J. Am. Chem. Soc.* **1969**, *91* (27), 7645–7647. https://doi.org/10.1021/ja50001a021.
(35) Fisher, E. M.; Pitz, W. J.; Curran, H. J.; Westbrook, C. K. Detailed Chemical Kinetic Mechanisms for Combustion of Oxygenated Fuels. *Proc. Combust. Inst.* **2000**, *28* (2), 1579–1586. https://doi.org/10.1016/S0082-0784(00)80555-X.
(36) Hurd, C. D.; Blunck, F. H. The Pyrolysis of Esters. *J. Am. Chem. Soc.* **1938**, *60* (10), 2419–2425. https://doi.org/10.1021/ja01277a035.
(37) Bilger, E. M.; Hibbert, H. Mechanism of Organic Reactions. IV. Pyrolysis of Esters and Acetals. *J. Am. Chem. Soc.* **1936**, *58* (5), 823–826. https://doi.org/10.1021/ja01296a043.
(38) Brezinsky, K. The High-Temperature Oxidation of Aromatic Hydrocarbons. *Prog. Energy Combust. Sci.* **1986**, *12* (1), 1–24. https://doi.org/10.1016/0360-1285(86)90011-0.
(39) Mackie, J. C.; Doolan, K. R.; Nelson, P. F. Kinetics of the Thermal Decomposition of Methoxybenzene (Anisole). *J. Phys. Chem.* **1989**, *93* (2), 664–670. https://doi.org/10.1021/j100339a033.
(40) Nowakowska, M.; Herbinet, O.; Dufour, A.; Glaude, P. A. Detailed Kinetic Study of Anisole Pyrolysis and Oxidation to Understand Tar Formation during Biomass Combustion and Gasification. *Combust. Flame* **2014**, *161* (6), 1474–1488. https://doi.org/10.1016/j.combustflame.2013.11.024.
(41) Togbé, C.; Tran, L. S.; Liu, D.; Felsmann, D.; Oßwald, P.; Glaude, P.-A.; Sirjean, B.; Fournet, R.; Battin-Leclerc, F.; Kohse-Höinghaus, K. Combustion Chemistry and Flame Structure of Furan Group Biofuels Using Molecular-Beam Mass Spectrometry and Gas Chromatography – Part III: 2,5-Dimethylfuran. *Combust. Flame* **2014**, *161*, 780–797.
(42) Djokic, M.; Carstensen, H. H.; Van Geem, K. M.; Marin, G. B. The Thermal Decomposition of 2,5-Dimethylfuran. *Proc. Combust. Inst.* **2013**, *34* (1), 251–258. https://doi.org/10.1016/j.proci.2012.05.066.
(43) Liu, D.; Togbé, C.; Tran, L. S.; Felsmann, D.; Oßwald, P.; Nau, P.; Koppmann, J.; Lackner, A.; Glaude, P.-A.; Sirjean, B.; et al. Combustion Chemistry and Flame Structure of Furan Group Biofuels Using Molecular-Beam Mass Spectrometry and Gas Chromatography – Part I Furan. *Combust. Flame* **2014**, *161*, 748–765.
(44) Meyer, J. A.; Stannett, V.; Szwarc, M. Conformational Analysis of Radical Abstraction of Hydrogen Atoms from Aromatic Hydrocarbons. *J. Am. Chem. Soc.* **1961**, *83* (1), 25–29. https://doi.org/10.1021/ja01462a004.
(45) Burgoyne, J. H. The Combustion of Aromatic and Alicyclic Hydrocarbons. I. The Slow Combustion of Benzene, Toluene, Ethylbenzene, N-Propylbenzene, N-Butylbenzene, O-Xylene, M-Xylene, P-Xylene and Mesitylene. *Proc. R. Soceity London. Ser. A, Math. Phys. Sci.* **1969**, *311* (1506), 445–467.
(46) Miller, L. L.; Nordblom, G. D.; Mayeda, E. A. A Simple, Comprehensive Correlation of Organic Oxidation and Ionization Potentials. *J. Org. Chem.* **1972**, *37* (6), 916–918. https://doi.org/10.1021/jo00971a023.
(47) Barresi, A. A.; Baldi, G. Deep Catalytic Oxidation of Aromatic Hydrocarbon

Mixtures : Reciprocal Inhibition Effects and Kinetics. *Ind. Eng. Chem. Res.* **1994**, 2964–2974.
(48) Haubrich, J.; Becker, C.; Wandelt, K. Adsorption and Interaction Energy of Ethene on Pt(1 1 1) and Pt Alloys: A Detailed Analysis of Vibrational, Energetic and Electronic Properties. *Surf. Sci.* **2009**, *603* (10–12), 1476–1485. https://doi.org/10.1016/j.susc.2009.01.045.
(49) Tsai, Y. L.; Xu, C.; Koel, B. E. Chemisorption of Ethylene, Propylene and Isobutylene on Ordered Sn/Pt(111) Surface Alloys. *Surf. Sci.* **1997**, *385* (1), 37–59. https://doi.org/10.1016/S0039-6028(97)00114-3.
(50) Delbecq, F.; Sautet, P. The Effect of Substituents on the Adsorption of Alkenes on (111) Pt and Pd Surfaces: A Theoretical Study. *Catal. Letters* **1994**, *28* (1), 89–98. https://doi.org/10.1007/BF00812473.
(51) Masclet, P.; Grosjean, D.; Mouvier, G.; Dubois, J. Alkene Ionization Potentials. Part I: Quantitative Determination of Alkyl Group Structural Effects. *J. Electron Spectros. Relat. Phenomena* **1973**, *2* (3), 225–237. https://doi.org/10.1016/0368-2048(73)80015-5.
(52) Sachtler, W. M. H. The Mechanism of the Catalytic Oxidation of Some Organic Molecules. *Chem.Rev* **1970**, *4* (December), 27. https://doi.org/10.1080/01614947108075484.
(53) Van Sickle, D. E.; Mayo, F. R.; Arluck, R. M.; Syz, M. G. Oxidations of Acyclic Alkenes. *J. Am. Chem. Soc.* **1967**, *89* (4), 967–977. https://doi.org/10.1021/ja00980a039.
(54) Mehl, M.; Vanhove, G.; Pitz, W. J.; Ranzi, E. Oxidation and Combustion of the N-Hexene Isomers: A Wide Range Kinetic Modeling Study. *Combust. Flame* **2008**, *155* (4), 756–772. https://doi.org/10.1016/j.combustflame.2008.07.004.
(55) He, J.; Wasa, M.; Chan, K. S. L.; Shao, Q.; Yu, J. Q. Palladium-Catalyzed Transformations of Alkyl C-H Bonds. *Chem. Rev.* **2017**, *117* (13), 8754–8786. https://doi.org/10.1021/acs.chemrev.6b00622.
(56) Battin-Leclerc, F. Detailed Chemical Kinetic Models for the Low-Temperature Combustion of Hydrocarbons with Application to Gasoline and Diesel Fuel Surrogates. *Prog. Energy Combust. Sci.* **2008**, *34* (4), 440–498. https://doi.org/10.1016/j.pecs.2007.10.002.
(57) Flaherty, D. W.; Uzun, A.; Iglesia, E. Catalytic Ring Opening of Cycloalkanes on Ir Clusters: Alkyl Substitution Effects on the Structure and Stability of C-C Bond Cleavage Transition States. *J. Phys. Chem. C* **2015**, *119* (5), 2597–2613. https://doi.org/10.1021/jp511688x.
(58) Flaherty, D. W.; Hibbitts, D. D.; Iglesia, E. Metal-Catalyzed C-C Bond Cleavage in Alkanes: Effects of Methyl Substitution on Transition-State Structures and Stability. *J. Am. Chem. Soc.* **2014**, *136* (27), 9664–9676. https://doi.org/10.1021/ja5037429.